University of Applied Sciences in Nowy Sącz

INDUSTRY 4.0 – developments and selected examples

edited by Grzegorz Przydatek

Scientific Editor

assoc. prof. Grzegorz Przydatek, PhD, Eng.

Reviews

prof. Józef Gawlik, PhD, Eng. prof. Marek Kułażyński, PhD, Eng.

Technical Editor

Tamara Bolanowska-Bobrek, PhD

© Copyright by Akademia Nauk Stosowanych w Nowym Sączu Nowy Sącz 2024

ISBN 978-83-67661-34-8

Publisher

Akademia Nauk Stosowanych w Nowym Sączu ul. Staszica 1, 33-300 Nowy Sącz tel.: +48 18 443 45 45, e-mail: sog@ans-ns.edu.pl www.ans-ns.edu.pl

Editor's adress

Wydawnictwo Naukowe Akademii Nauk Stosowanych w Nowym Sączu ul. Staszica 1, 33-300 Nowy Sącz tel.: +48 18 443 45 45, e-mail: wn@ans-ns.edu.pl, tbolanowska@ans-ns.edu.pl wydawnictwo.ans-ns.edu.pl

Printing

Wydawnictwo i drukarnia NOVA SANDEC s.c. Mariusz Kałyniuk, Roman Kałyniuk ul. Lwowska 143, 33-300 Nowy Sącz tel.: +48 18 441 02 88, e-mail: biuro@novasandec.pl

Contents

THE USE OF HYDROGEN IN TRANSPORT – COMBUSTION, ENGINE DURABILITY AND ENVIRONMENTAL PROTECTION (Arkadiusz Kamiński, Janusz Jakóbiec, Bogusław Cieślikowski)	5
DESTRUCTION OF FUNCTIONAL SYSTEMS OF A DIESEL ENGINE	,
RESULTING FROM THE FORMATION OF PM DEPOSITS (Bogusław Cieślikowski)	5
LONG-TERM FORECASTING IN TECHNICAL FACILITIES MANAGEMENT SYSTEMS (Jerzy Korostil)	5
APPLICATION OF CHROMATOGRAPHIC SEPARATION	J
METHODS IN QUALITATIVE DATA ANALYSIS FOR SELECTED DATA SETS (Mariusz Święcicki)	7
AUTOMATION AND INTEGRATION OF PRODUCTION SYSTEMS IN A MIXED MANUFACTURING ENVIRONMENT –	
USING FAKRO AS AN EXAMPLE (Wojciech Klimek)	3

THE USE OF HYDROGEN IN TRANSPORT – COMBUSTION, ENGINE DURABILITY AND ENVIRONMENTAL PROTECTION

Arkadiusz Kamiński¹, Janusz Jakóbiec², Bogusław Cieślikowski³

Abstract: The paper describes the challenges for the transport sector resulting from the energy transformation of this part of the economy in the face of megatrends. Ongoing research and analyses indicate that to achieve the emission reduction goals during the transition period, it is reasonable to consider an alternative in the form of hydrogen-powered internal combustion piston engines as the driving force of transport vehicles. This is related to promoting the decarbonization of fuels to combat climate change. Zero- and low-emission hydrogen-based fuels may be the key to meeting global and European sustainability and climate goals. Conventional ICE engines, although widely used, require further research in the field of hydrogen power in the area of technology, method of powering and combustion as well as proper operation to ensure durability. HICE combustion engines do not have to compete with fuel cell technology. They can constitute complementary technologies in terms of contributing to reducing of greenhouse gas emissions, ensuring safe transport of people and goods, which is necessary for the development of civilization.

Keywords: hydrogen, transport, energy carriers, emissions.

Introduction

Transport is important to both the economy as a whole and people's daily lives. Between 1970 and 2020, the world's population doubled, and the rate of urbanization increased by 50% (Deloitte, 2018). Projections by the United Nations, based on data collected by the Food and Agriculture Organization (FAO) and the World Water Council, assume that by 2050 the world's population will increase by 1/3, which will translate into an increased rate of the population's movement to cities. Cities will play a key role as engines of the global economy. More than 8 billion people live on Earth, and the UN forecasts that this number will increase to 11 billion by 2100 (FAO, 2022; UN DESA, 2022). According to the International Energy Agency, the European Automobile Manufacturers' Association, data publisher Statista and automotive industry analysts JATO Dynamics, the world's population has around 1.475 billion cars.

The process of urbanization indicates that today's cities are the main centers where more and more transport needs arise. This results in an increase in freight and passenger traffic, which in turn contributes to an increase in environmental and noise pollution, accidents, and thus a deterioration in the quality of life in cities. Energy carriers in the form of fossil fuels such as oil, coal and gas are of great importance to the development of humanity. On the one hand, human activities based on the combustion and use of fossil fuels have led to significant anthropogenic CO₂ emissions into the

ORLEN S.A., Chemików 7, 09-411 Płock, Poland; e-mail: arkadiusz.kaminski@orlen.pl

² University of Applied Sciences in Nowy Sacz, Faculty of Engineering Sciences, Zamenhofa 1A, 33-300 Nowy Sacz, Poland; e-mail: jjakobiec@ans-ns.edu.pl

³ University of Applied Sciences in Nowy Sacz, Faculty of Engineering Sciences, Zamenhofa 1A, 33-300 Nowy Sacz, Poland; e-mail: bcieslikowski@ans-ns.edu.pl

atmosphere, but, on the other hand, these natural resources have improved the quality of life of billions of people around the world by providing available, relatively inexpensive energy and raw materials for all types of production of goods and services. A major challenge for European transport policy is to reconcile the increasing demand for transport services with the decreasing availability of resources and environmental constraints. It is important to note the high level of correlation between economic growth and freight-passenger transport volumes.

Forecasts by the International Transport Workers' Federation (ITF) indicate an increasing demand of between 134 and 363% in international freight transport by 2050, and a corresponding increase in CO₂ emissions of between 94 and 163%, depending on the environment in which it is carried out through maritime, road, rail, inland waterway and air transport (OECD, 2019).

The European Commission's strategy to achieve climate neutrality by 2050 is to reduce the use of fossil fuels and improve air quality, especially in cities. One of the ways to achieve this goal is to decarbonize the economy, including the transport sector, which is crucial for companies in global supply chains. From a formal and legal point of view, the Trans-European Transport Network (TEN-T) is gaining importance as an instrument for coordinating and ensuring coherence and complementarity of infrastructure investments. In addition, intelligent transport systems are also an integral component of the project, the implementation of which contributes to the improvement of network capacity, traffic safety and the reduction of environmental pollution caused by transport.

A European strategy for sustainable and smart mobility is therefore essential. In January 2020, the Parliament adopted a resolution on the European Green Deal, responding to the European Commission's communication and providing some guidance on transport in the document "Accelerating the transition to sustainable and smart mobility" (EC, 2020; EC, 2022a,b).

Many experts believe that zero- and low-emission hydrogen used in hydrogen fuel cell electric vehicles is the key to handling this challenge, in both passenger and heavy duty transport, covering land, sea and air. Still, most hydrogen is currently being used for fossil fuel processing and its use has become widespread in oil refining and ammonia production, mainly for the fertiliser market. An integral part of the energy industry since the mid-20th century, hydrogen can be used in vehicles in two ways: either as a fuel in a hydrogen engine or by converting it to electricity using a fuel cell and then using this electricity in an electric motor that is part of the drivetrain.

Scientists have been studying hydrogen with great interest for years because of its potential as a pollution-free fuel. Hydrogen is a carbon-free energy carrier so during the combustion process only water is produced, making it a clean fuel with no emissions. Hydrogen is a low-carbon energy carrier that has great potential to decarbonise carbon-intensive sectors. Although hydrogen is colourless, the different ways of producing hydrogen are divided by colour. The majority of hydrogen produced today is 'grey' and is created by decomposing natural gas into hydrogen and carbon dioxide, while the latter is released into the atmosphere. According to the International Energy Agency (IEA), hydrogen and hydrogen-based fuels could meet 10% of the global energy demand and reduce cumulative emissions by 6% under the IEA Net Zero by 2050. Ultimately, hydrogen could help ensure energy security and play an important role in the energy transition to low-carbon fuels (IEA, 2022).

1. Methodology

The paper is a review article based on a problem study and an analysis of selected literature, including global policies, trends and internet sources. The article presents the impact of hydrogen combustion in engines in terms of their emissions and durability. It analyses the feasibility of using conventional hydrogen-fuelled engines for transition to a low-carbon economy in order to achieve sustainable development goals, climate neutrality and, at the same time, provide access to the free movement of goods and services.

The paper attempts to highlight conventional ICE engines in the context of the need to meet not only the UN Sustainable Development Goals, but also the challenges of climate policies, the Paris Agreement and the Fit for 55 package in the face of the world's growing population. The focus of the paper is on the transport sector emitting carbon dioxide and other substances into the atmosphere. Undoubtedly, the energy transition and the type of energy carriers used will have an impact on greenhouse gas emissions, access to energy forms and carriers, and energy security.

2. Legal aspects of environmental protection in transport

Transport generates around 55% of the EU's GDP and employs more than 10 million people in Europe (Gis 2018). There are around 413 million cars in Europe. According to Eurostat and the European Automobile Manufacturers' Association (ACEA), there were 253.3 million passenger cars registered in the European Union in 2021. According to IEA data, greenhouse gas emissions from transport in 2021 stood at 8.5 GMgCO2e (gigatonnes of CO₂ equivalent), or about 21% of all global emissions estimated at 33.3 GMgCO2e (IEA, 2022; Sen, Miller, 2022). The biggest challenge is emissions from road transport, which accounts for three-quarters of transport emissions and thus 15% of all global greenhouse gas emissions – GHG (*Green House Gases*). Passenger transport (cars, motorcycles, buses, and coaches) accounts for 9% of all greenhouse gases entering the atmosphere each year (IEA, 2022). According to the European Environment Agency (EEA), around 25% of the EU's total CO2 emissions in 2019 came from the transport sector, 71.7% of which came from road transport (IEA, 2017a,b; IEA, 2020a,b,c,d,e; OECD, 2020; UNFCCC, 2020; European Parliament, 2022). Emissions from road transport in Poland in 2019 stood at approximately 63,000 Gg (KOBiZE, 2021).

2.1. Environmental challenges

The operational requirements for fuels are changing (Kamiński, 2014, 2015), which in turn is related to the problems of the environmental impact of fuels in their life cycle (Life Cycle Assessment) or the so-called cycle from source to tank (Keesom et al., 2012; Rogowska et al., 2014). The change in fuel composition is subject to modifications, mainly as a result of measures to reduce atmospheric air pollution and contamination of ground-water with harmful substances from the combustion of petroleum fuels and progress in the development of engine design and technology (Kamiński et al., 2018 a, b; Kamiński et al., 2019; Jakóbiec et al., 2021; Kamiński et al., 2021; Pusz, Kamiński, 2023). These actions force designers of motor vehicles to make changes in the design of power supply systems, engine compartments, and exhaust gas treatment systems. Fuel manufacturers have to adjust their product quality to the requirements of car designers to minimize the emission of harmful substances generated during fuel combustion.

In the literature, one can find views on the comprehensive assessment of the environmental hazard caused by the use of motor vehicles (Scott et al., 2014; Burchart-Korol, 2017; Khan, 2018). One can read about the methods of analysis of emissions, pollutants harmful to the environment and energy inputs at the stages of production and distribution of energy carriers from the source of energy carrier to the fuel tank (Well-to-Tank) and the use of vehicles from the fuel tank to the wheel of the vehicle (Tank-to-Wheel). In these cases, the Eco-inicator 99 procedures and the Swiss Ecological Scarcity Method, also known as the Ecoscarcity method or UBP'06 (Goedkooop 2001), are mainly used. Balancing environmental hazards throughout the contractual life cycle of a motor vehicle is usually carried out using a specific method and appropriate software (due to the large amount of data and sometimes complex calculation algorithms).

The area of application of the analysis of the so-called WtW (Well-to-Wheel) is the determination of pollutant emissions, most often greenhouse gases (GHG) and energy consumption associated with the use of various types of fuels and the corresponding possible vehicle drives. This takes into account the entire contractual life cycle of the fuel, including the extraction of primary energy carriers, their conversion into energy carriers used to power the vehicle, transport and distribution, and the final emission of pollutants from the vehicle during its operation. In practice, Well-to-Wheel analysis is carried out in two stages (Edwards, 2011):

- from the source of the energy carrier to the fuel tank (WtT);
- from the fuel tank to the vehicle wheel (TtW).

The final result is the sum of energy consumption and the sum of pollutant emissions (GHG) determined at both stages. Energy losses and pollutant emissions resulting from fuel preparation depend on many factors, not only on the type of fuel used, the production method adopted, the substrate used and the method of energy supply adopted, but also on other infrastructure indirectly related to production.

Figure 1 shows global CO₂ emissions from transport under the IEA Sustainable Development Scenario up to 2070 across different components of the transport sector.

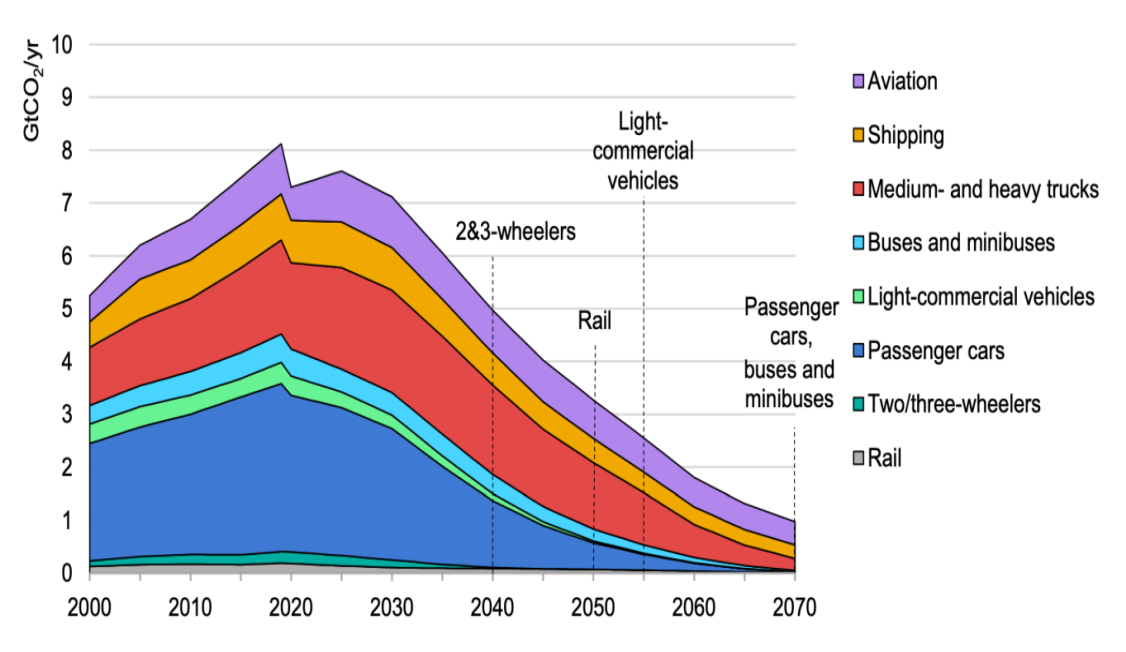


Figure 1. Global CO₂ emissions from transport in the IEA Sustainable Development Scenario up to 2070 (IEA, 2020f).

The IEA report (IEA 2020f) on the energy technology perspective presents a "Sustainable Development Scenario" for achieving net-zero CO₂ emissions from the transport sector by 2070. With electrification and hydrogen technologies, some of these sub-sectors could decarbonise within decades. The IEA's scenario calls for emissions to be phased out from motorcycles by 2040, from railways by 2050 and from small trucks by 2060, and while emissions from cars and buses will not be eliminated by 2070, several countries, including the European Union, the United States, China and Japan, are expected to phase out conventional vehicles as early as 2040. Thus, despite reducing emissions by up to three quarters in the visualized scenario, emissions from these subsectors will continue to be the largest source of transport-related emissions in 2070. To achieve net-zero for the sector as a whole, these emissions need to be offset by 'negative emissions' (e.g. carbon capture and storage from bioenergy or direct air capture) from other parts of the energy system.

2.2. European transport policy

Transport policy has been one of the EU's common policies for over 30 years. Besides opening up transport markets to competition and creating trans-European networks, the sustainable mobility model will become increasingly important, not least because of the steady increase in greenhouse gas emissions in this sector, which may undermine the completion of the European Union's climate objectives. The 2011 White Paper "Roadmap to a Single European Transport Area – Towards a Competitive and Resource Efficient Transport System" (EC 2011) recommends a 20% reduction in transport emissions (excluding international maritime transport) in the period 2008-2030 and at least a 60% reduction in transport emissions between 1990 and 2050. It also aimed to reduce emissions from international maritime transport by 40% between 2005 and 2050. It proposes that 40% of aviation fuels should be sustainable low-carbon fuels by 2050. It advocates halving the number of conventionally powered cars in urban transport by 2030 and phasing them out completely by 2050. However, these targets were too low compared to the targets set at the Paris climate conference in December 2015 (also known as 'COP 21'). This circumstance had an impact on the action plan proposed by the Commission (EC 2019) "European Green Deal", which goes beyond the main ambitions (such as "smart and sustainable mobility") and also takes into account the overarching objectives of climate law, thus transforming political commitments on climate policy into legal obligations. In December 2020, the European Commission presented a Sustainable and Smart Mobility Strategy with an action plan with 82 initiatives to guide work up to 2024 (EC 2020). The strategy sets out a roadmap to put European transport firmly on the right track towards a sustainable and smart future, and identifies 10 flagship areas broken down by milestones. One of these milestones is to reach at least 30 million zero-emission cars on the road by 2030. In July 2021, the European Commission put forward several proposals and legislative reviews in the area of decarbonising transport in line with the Green Deal's objective of achieving climate neutrality by 2050. In line with the objectives of the European Green Deal and following the publication of the Sustainable and Smart Mobility Strategy in December 2020, the Commission presented a second package of proposals in December 2021 to support the transition to cleaner, greener and smarter transport. The package consisted of two important legislative proposals: the revision of the 2013 TEN-T Guidelines Regulation and the 2010 revision of the Intelligent Transport Systems (ITS) Directive.

The European Green Deal commits the sector to a 90% reduction in greenhouse gas emissions from transport in order to make the EU a climate-neutral economy by 2050, while also aiming to achieve zero pollution. To achieve this systemic change, Europe needs to make all modes of transport more sustainable and ensure that sustainable alternatives are widely available in the transport system and put in place the right incentives to support the transition.

Despite an ambitious transport policy, there were years of steadily increasing greenhouse gas emissions from the EU transport sector; it was not until 2020 that the emissions decreased significantly due to limited activity during the COVID-19 pandemic. Preliminary estimates of emissions in 2021 indicate an increase in transport emissions of 8.6%, followed by a further increase of 2.7% in 2022. National projections by the European Environment Agency (EEA) suggest that even with the actions currently planned by the Member States, national transport emissions will not fall to the 1990 levels until 2032. Emissions from international transport (aviation and sea) are projected to continue to rise.

3. Motor vehicles and energy carriers

On the one hand, the requirements for vehicles, including motor vehicles, in terms of low fuel consumption, reliability, emissions and environmentally friendly operation are becoming more and more demanding, which translates into actions taken to improve the thermal efficiency of engines, to reduce friction and wear and tear in drive units, to measure emissions in real conditions, to multi-directionally reduce particulate emissions and to match the right engine to the right car, the so-called rightsizing. This, in turn, translates into the search for low-emission fuels, alternative fuels and e-fuels.

To reduce emissions, the vehicle sector is introducing, among other things, internal combustion engines powered by fuels with bio-components, internal combustion engines powered by synthetic fuels, hybrid powertrains and internal combustion engines powered by hydrogen, and internal combustion engines powered by ammonia. For hydrogen-powered engines, hydrogen can be used in both spark-ignition (SI) engines as well as compression ignition (CI) engines. Solutions which are used in spark-ignition engines consist in the induction of hydrogen into the manifold (CVI, EFI), direct introduction (DI) or the addition of hydrogen to gasoline, i.e. mixing it with conventional fuels. Exhaust gas recirculation is also used to improve the performance of hydrogen-powered engines. The challenges of atypical combustion remain to be solved by correlating the synergies of injection and ignition strategies.

3.1. The history of hydrogen-powered vehicles

The history of hydrogen-powered vehicles is long and dates back to the first half of the 19th century. A hydrogen vehicle is a vehicle that uses hydrogen fuel for propulsion. Energy is produced by converting hydrogen's chemical energy into mechanical energy, either by reacting hydrogen with oxygen in a fuel cell to power electric motors, or, less commonly, by burning hydrogen in an internal combustion engine.

The first vehicle with an internal combustion engine (ICE) powered by hydrogen was made using a balloon filled with hydrogen and oxygen by the Swiss inventor Francois Isaac de Rivaz in 1807. Technically, it could be called the first hydrogen car, although the first modern hydrogen-powered vehicle did not appear until more than

150 years later. The inventor of the fuel cell is considered to be the chemist, lawyer and physicist William Grove, who in 1847 invented a working fuel cell, a device that converted the chemical energy of hydrogen and oxygen into electricity. Its work was expanded by English engineer Francis Thomas Bacon between 1939 and 1959, and the first modern fuel cell vehicle was the Allis-Chalmers farm tractor, which was equipped with a 15 kW fuel cell in the late 1950s. The first road vehicle to use a fuel cell was the Chevrolet Electrovan, which was built in 1966 at General Motors and boasted a range of nearly 200 km and a top speed of 112 km/h. In the following years, hydrogen was mainly used as a fuel source for space shuttles in the 1980s and 1990s. Between 2005 and 2007, BMW tested the BMW Hydrogen 7 luxury car, powered by a hydrogen ICE engine that reached a speed of 301 km/h in tests. This technology was used in the Aston Martin Rapide S during the Nürburgring 24-hour race. Verhelst and Sierens (Verhelst, Sierens, 2001) upgraded the GM/Crusader V8 engine from traditional fuels to hydrogen for the sole purpose of testing its capabilities in public transport buses. The engine was equipped with a lower fuel injection system that delivered hydrogen at a pressure of 3 bars. The compressed hydrogen was stored in steel bottles at a pressure of 200 bars. Sopena et al. (2010) modified an ICE engine powered by gasoline with ZI ignition in a transport vehicle (bus) to run solely on hydrogen fuel. The most important modifications were to the electronic control unit, gas injectors, intake manifold, and oil cooler. MAN wants to refine and incorporate the technology developed in the 1990s. The hydrogen engines were intensively tested in MAN buses in Berlin between 2006 and 2009. MAN hydrogen-powered buses have been in operation in Berlin since 2006. The MAN Lion's City Hydrogen in Berlin has an engine output of approx. 180 hp (130 kW). The maximum speed of the vehicle is 82 km/h, and the range on a single hydrogen tank is 200 kilometers. The buses were deployed as a showcase of Berlin during the Football World Cup in Germany. The hydrogen engines used were a development of the prototype hydrogen buses tested in Munich between 1996 and 1999.

3.2. Fuels as energy carriers

In order to meet the requirements related to emissions, new types of fuels are being introduced, e.g. synthetic fuels called e-fuels. These are fuels produced in the process of synthesis using renewable electricity, often using inorganic raw materials (RFNBO fuel). E-fuels include liquid and gaseous hydrocarbons such as methane and other gasoline-like fuels, diesel, alcohols such as ethanol and methanol, and carbon-free fuels such as hydrogen and ammonia. Once the refining process is complete, the produced e-fuels can be used as e-gasoline, e-diesel, e-heating oil, and e-kerosene. The only e-fuel for ZI engines that meets the requirements of a second-generation synthetic fuel for full combustion without the formation of soot particles, and without harm to the environment and health, is a mixture of dimethyl carbonate (DMC) and methyl formate (MF), called DMC+. The currently produced synthetic fuels, including e-fuels, must meet the requirements of EN 228 or EN590. In such a situation, they are referred to as "drop-in" fuels, i.e. they can be directly used in current combustion engines as intrinsic fuels or as admixtures to conventional hydrocarbon fuels (Stępień, 2023).

The International Energy Agency is identifying hydrogen-based synthetic fuels as a potential solution to reduce aviation emissions. Hydrogen-based biofuels have the potential to enable the aviation sector to fly on a larger scale and to fly longer without emissions. Emission-free hydrogen, as previously mentioned, could become the main fuel in modes of transport such as trains, trucks and cars.

3.3. Characteristics of hydrogen-powered vehicles

Hydrogen can be used in vehicles in two ways: as a fuel in a hydrogen engine or by converting it into electricity using a fuel cell. Hydrogen engines burn hydrogen in an internal combustion engine in the same way as conventional engines burn gasoline. Hydrogen ICE (HICE) engines are almost identical to traditional spark-ignition engines. Internal combustion engines are usually most efficient under heavy load. Hydrogen engines can often run on lower quality hydrogen without having to purify it. The hydrogen engine's resistance to pollution is also useful in the transportation industry, where the transition to green, high-quality hydrogen will take time. Vehicles equipped with hydrogen combustion engines can operate without CO₂ emissions from hydrogen fuel, either directly or indirectly, depending on the source of hydrogen used. Additionally, hydrogen fuels do not emit particulate matter, carbon monoxide, or volatile organic compounds. However, hydrogen engines can emit a certain amount of NOx. To eliminate most NOx emissions, exhaust aftertreatment systems are used. Hydrogen combustion engines emit directly less NOx than comparable compression ignition engines. The formation of nitrogen oxides during hydrogen/air combustion can be minimized with excess air. NOx emissions can also be reduced by cooling the combustion environment using techniques such as water injection, flue gas recirculation or the use of liquid hydrogen. NOx and CO₂ emissions have been detected in hydrogen engines as a result of lubricating oil (in hydrogen engines they are typically one order of magnitude lower than emissions from comparable gasoline engines [Norbeck et al., 1996]). However, the use of hydrogen in internal combustion engines results in a loss of power due to the lower energy content of the stoichiometric mixture in the engine cylinder. A stoichiometric mixture of gasoline and air and hydrogen gas and air, pre-mixed externally, occupies \sim 2% and 30% of the cylinder volume respectively. Under these conditions, the energy of the hydrogen mixture is only 85% of the hydrogen mixture, resulting in about a 15% reduction in power. Therefore, the same hydrogen-powered engine will have ~15% less power than a gasoline-powered one. The power output of a hydrogen engine can be increased by using more advanced fuel injection techniques or liquid hydrogen. For example, if liquid hydrogen is pre-mixed with air, the amount of hydrogen that can be introduced into the combustion chamber can be increased by about one-third (Norbeck et al., 1996). To compensate for the loss of power, hydrogen engines are usually larger than gasoline engines and/or are equipped with turbochargers or superchargers. The low ignition energy and rapid spread of hydrogen flames have led to some challenges with pre-ignition and backfire. These problems are solved by adding hydrogen to the air mixture at a time when pre-ignition conditions are less likely, e.g. separate fuel and air supply to the combustion chamber and/or injecting pressurized hydrogen into the combustion chamber before the piston is in the top dead center and after the air valve is closed. Water injection and exhaust gas recirculation techniques are also used in hydrogen engines to help control pre-ignition. It should be noted that most of the

research on hydrogen combustion in internal combustion engines has been carried out with modifications of existing engines designed to burn gasoline. Redesigning the combustion chamber and cooling systems to take into account the unique combustion properties of hydrogen may be the most effective method to address the problems of pre-ignition and knocking (Norbeck et al., 1996; Agardy et al., 2005).

4. Review of the literature on research on hydrogen powered engines

Hydrogen has the potential to become the sustainable fuel of the future, to reduce global dependence on fossil fuel resources and to reduce emissions from the transport industry. As a result, research is being carried out in the field of hydrogen-powered transport engines to assess the feasibility of using hydrogen as the main fuel of the future. Research by Agardy et al. (2005) showed that hydrogen has the potential to become the sustainable fuel of the future, to reduce global dependence on fossil fuel resources, and to reduce emissions from the transport industry. At the same time, the authors highlighted the use of hydrogen as an additive to hydrocarbon fuel systems to achieve higher performance than hydrogen-only internal combustion engines. Using a dual-fuel strategy can increase combustion stability and thermal efficiency, reducing CO₂ and unburned hydrocarbon emissions and fuel consumption.

On the other hand, a study conducted by Garrett (2010) with Argonne National Laboratory to determine the reliability of HICE engines found that the technology provided reliability during operation and during the project lifetime, and that analyses of engine components (including oil) showed little sign of wear or stress, with the exception of valves and cylinder head seats. Analysis of the material of these components showed signs of hydrogen embrittlement of the intake valves. Quite large carbon deposits were observed on the surfaces of the intake and exhaust valves and piston crowns in HICE units. They were the result of excessive engine oil ingress due to the high oil level of boost pressure. The data from the experiment showed that this technology can provide reliably low exhaust emissions through careful engine calibration and without additional exhaust gas treatment. This work identified specific areas and components where additional research could benefit from further improving the durability of HICE engines.

Bai-gang et al. (2014) investigated different combustion time characteristics of hydrogen in HICE through experiments and analysis of the physical properties of hydrogen compared to gasoline. A diagram of the pressure increase rate as a function of the crankshaft rotation angle at 4,000 rpm showed the proportional relationship between the richness of the mixture, the peak pressure in the cylinder and the rate of pressure increase, which depend on the combustion speed. Due to hydrogen's wide flammability range and low ignition energy, rapid combustion of the hydrogen-air mixture in ICE is inevitable; therefore, unwanted backfire and pre-ignition should be controlled (Duan et al., 2014). Wang et al. (2017) proved that nozzle position did not have a significant effect on the homogeneity of the hydrogen-air mixture in HICE; however, the greater distance between the inlet valve and the nozzle increased the likelihood of backshot. The optimal position of the nozzle will be closest to the inlet valve. At the current stage of research, the use of hydrogen as an additive to hydrocarbon fuels in ICE engines is a method that can encourage the use of hydrogen in transport engines (Juste, Benavides, 2008; Tartakovsky, Sheintuch, 2018).

Barbira et al. (2016) pointed out in a comprehensive study that the topic of hydrogen as a fuel for internal combustion engines has been a topic of research for over a hundred years. There is now a resurgence of interest in hydrogen fuel due to its ability to provide long-term solutions to energy and environmental crises. Numerous studies of hydrogen engines have been carried out in different parts of the world. Technical solutions to counteract the characteristic problems leading to pre-ignition, back-ignition, uneven combustion and high pressure build-up rates are discussed. The technological side of the operation of spark-ignition (SI) and compression ignition engines on hydrogen fuel is presented in order to obtain optimal performance and low exhaust emission characteristics without undesirable combustion phenomena. In the case of ZI engines, fuel induction techniques are the most important part of the system's development. The design features of fuel suction techniques in ZI engines are discussed to achieve optimal engine configuration. The technical features of hydrogen supplementation and the potential of hydrogen-blended fuels were highlighted. The differences between a conventional engine and a hydrogen-powered engine are discussed. The study also highlights the prospects and market potential of the current hydrogen-powered engine and analyses the emerging trend towards its market penetration. It was pointed out that hydrogen, as a zero-emission fuel, makes it possible to build a reciprocating internal combustion engine, which can be classified as a drive for zero-emission vehicles in terms of CO₂ emissions. Thus, the hydrogen-powered reciprocating internal combustion engine could be a future transition technology in powertrains, especially in trucks and off-road vehicles, competitive with both electric drives and fuel cells. The article presents a multidirectional analysis of the prospects for the development and dissemination of hydrogen-powered internal combustion piston engines in motor vehicles. The current interest of the automotive industry in hydrogen-powered combustion engines, the current state of their development and the challenges that need to be overcome are presented. The article also points out the various conditions that will determine the future of these engines in Europe.

Research by Hoseini and Butler (2020) indicates that the use of HICE motors can achieve efficiencies of 20-25%. Due to technical barriers in HICE, the possibility of using hydrogen as an additive to hydrocarbon fuels, as a transitional solution to reduce greenhouse gas emissions in transport engines, has been developed.

As Rezaei et al. (2021) point out, one of the challenges for the transport sector is to reduce greenhouse gas emissions. In the EU and the USA, there is a trend that cannot grow by merely optimizing vehicles and engines. Hydrogen fuel, which can be produced from biomass or renewable energy such as solar and wind power, is considered one of the key energy solutions to reduce CO₂ emissions in the transport sector. Using numerical simulation, confirmed by measurements of single-cylinder engines, Rezaei et al. noted pre-ignition and glow ignition resulting from the very short delay time of hydrogen auto-ignition at high mixture temperatures and the low ignition energy requirement of hydrogen.

Stępień (2021) summarized the experiences and opinions of various international research centers on the technical feasibility of using hydrogen as a fuel in ICE engines. He critically reviewed the concept of hydrogen combustion, drawing on the results of previous research and experiments described in a number of scientific papers. He devoted a lot of space to discussing the challenges and opportunities related to port and direct

hydrogen injection technology. A comparison of different fuel injection and ignition strategies and the benefits resulting from the use of synergy of selected solutions are presented. Reference was made to the previous experience of various research centers, and the risks associated with abnormal hydrogen combustion, such as pre-ignition, late pre-ignition, knocking and back-ignition, were described. Attention was drawn to the fundamental importance of optimizing the composition of the air from the point of view of combustion quality, NOx emissions, efficiency and engine performance. Cleaning up the exhaust gas to meet future emissions regulations for hydrogen-powered internal combustion engines is another issue under consideration. The article also discusses the modifications necessary to adapt the existing engines to work on hydrogen. Addressing the still unresolved issues, the reliability challenges faced by fuel injection systems are presented in particular. An analysis of more than 150 papers shows that hydrogen is a suitable alternative fuel for spark-ignition engines. This will significantly improve their efficiency and significantly reduce emissions to a fraction of their current levels. However, its use also has some drawbacks, the most important of which are high NOx emissions and low power output, as well as problems related to the durability and reliability of hydrogen-powered engines.

Onorati et al. (2022) found that an internal combustion engine powered by H₂ is a viable alternative to the powertrain of vehicles without causing CO₂ emissions. High boost pressures, direct injection, advanced combustion modes, the use of laser ignition and dedicated SCR exhaust after treatment systems will guarantee competitive high-efficiency drive technology. Given the possible development of the next generation of HICE, the resulting thermodynamic efficiency will be similar to that of a modern fuel cell powertrain.

Falfari et al. (2023) highlighted that hydrogen has the potential to be the fuel of the future for internal combustion engines, primarily because it is the only one with low NOx emissions (which are almost zero at low/medium loads) and zero HC and CO₂ emissions. The authors pointed to a challenge related to the oil particle problem (related to the properties of hydrogen) that needs to be addressed at the piston-liner clearance design stage. The main challenges of using hydrogen as a fuel in spark-ignition engines are:

- elimination of abnormal combustion (Direct injection of hydrogen gas into the combustion chamber reduces the risk of backfire and pre-ignition in the intake manifold. The use of dilute mixtures of hydrogen and air eliminates the risk of detonation, or knocking.);
- management of pre-ignition in hot areas around the spark plug (It is necessary to use cooled spark plugs or unconventional ignition systems based on the corona effect. Such unconventional ignition systems are suitable for ignition of very dilute hydrogen-air mixtures.);
- Definition of the optimal injector layout and shape (number of holes, diameter and relative position on the injector tip).

Hydrogen can be used in a compression ignition (CI) engine. It has been found that the power generated by a CI motor is twice as much as the power generated by the same motor operating in a pre-mixed system (Ganesan, 2012). In hydrogen-powered CI engines, an injector is used to inject hydrogen at high pressure into the cylinder (Naber, Siebers, 1998). Therefore, what is important is not only the design of the engine structure, but also the design of the injector, since the injection nozzle controls how

pressurized hydrogen is injected into the system (Gomes Antunes et al., 2009). Hydrogen supply in CI engines has shown a significant reduction in the level of CO₂, CO and HC; the reduction can reach even more than 50% under optimal conditions. A visible effect of the use of large amounts of hydrogen in internal combustion engines (high load conditions) is a rapid increase in the rate of heat release, and consequently an increased temperature in the cylinders and a high rate of NOx formation (Dimitriou, Tsujimura, 2017). Szwaja and Grab-Rogaliński (2009) used pure hydrogen in a homogeneous charge compression ignition (HCCI) engine. To achieve hydrogen auto-ignition in HCCI mode, a compression ratio of at least 16 was used. It was found that the use of a stoichiometric hydrogen-air mixture in HCCI mode generates extremely high knocking. Therefore, to reduce the knocking effect, various methods such as lean combustible mixture or EGR (exhaust gas recirculation) must be used.

In addition to modifying the combustion process itself, EGR has been used to improve the performance of hydrogen-only engines. To investigate the effect of EGR on pollutant formation and combustion characteristics at different proportions of hydrogen, Du et al. (2017) used an engine with gasoline injection into the intake port and hydrogen DI (direct injection). The experiments showed that when a small amount of hydrogen was added to the combustion process, the peak pressure in the cylinder increased by 9.8% and the engine torque – by 11%. The use of a 20% EGR ratio and a 5% hydrogen ratio improved the engine's torque output by about 20% and reduced NOx generation by 54.8% compared to the original engine without the addition of hydrogen. Also, CO₂ and hydrocarbon emissions have been significantly reduced by adding hydrogen to the system. It has been found that the co-control of EGR and the addition of hydrogen in the engine significantly reduces fuel consumption. A similar test was carried out by Fennell et al. (2014) modifying a conventional EGR system to a reformed exhaust gas recirculation (REGR) system to improve the efficiency of the gasoline DI system. The results showed that REGR improved engine efficiency compared to a gasoline engine, and REGR outperformed EGR due to the extended dilution limit. REGR greatly reduced NOx formation and moderately increased HC emissions. Both EGR and REGR reduced or eliminated knocks, as well as reduced particulate matter and mass emissions.

The use of liquid hydrogen is another method that does not require significant changes to conventional ICEs. In this system, liquefied hydrogen is injected into an expansion chamber to be converted into cold hydrogen gas and is finally directed to the combustion chamber. The use of cold hydrogen reduces NOx emissions (Gurz et al., 2017). In the early 2000s, Peschka investigated DI and PFI (port fuel injection) direct injection methods for HICE. DI provides high efficiency and controlled emissions, but the durability of DI injectors is low. Injection requires high pressure, which further limits storage options. Hydrogen can be stored in cryogenic tanks in a liquid state, and injection pressure is generated on board or compressed hydrogen is stored, which limits tank capacity, and onboard compression would diminish DI performance benefits (Peschka, 1998).

The current and, in particular, future targets for drastic reductions in CO₂ emissions in the short term (in the EU, the "Fit for 55" package) are already a major challenge for the automotive industry. The use of hydrogen to power reciprocating combustion engines is becoming more and more popular because it does not contain any carbon compounds and does not cause CO₂ emissions during combustion. Piston combustion engines can be used both in motor sports and passenger cars (Toyota), as

well as in trucks (MAN, Deutz, Cummins) and off-road machines (JCB). Current research into advanced hydrogen-powered internal combustion engines is focused on achieving thermal efficiencies higher than 45% while maintaining low NOx emissions. To achieve these goals, modern hydrogen-powered internal combustion engines use direct fuel injection (DI) strategies. However, the proliferation of hydrogen-powered internal combustion engines presents several challenges, the most important of which are:

- further development of injection and mixture and ignition strategies;
- simultaneous optimization of supply, ignition and combustion process strategies to avoid abnormal combustion processes;
- solving material problems related to the harmful effects of hydrogen on materials;
- solving lubrication problems the right lubricating oil;
- adapting the design of engines and cooperating systems to operate on hydrogen fuel.

When hydrogen is used as a fuel for reciprocating internal combustion engines, lubrication problems need to be solved. Antonioli and Vassallo (Sosa, 2022) stated that in the field of lubricant technology for HICE, sustainability will play an increasingly important role compared to today, ranging from recycled lubricants and bio-lubricants to e-lubricants (synthetic oils obtained from CO₂ capture and renewable electricity. The authors anticipate the need for the oil to be compatible with the aftertreatment system, which HICE may need for some heavy-duty lean-burn applications that comply with very stringent environmental standards. They are convinced that the oil that will be used in HICE engines should be formulated in such a way that it is backward compatible with existing engines, thus facilitating the successful commercial introduction of this new sustainable powertrain.

In his research, Falfari (2023) pointed out two significant challenges with HICE engine lubrication. The first one concerns the very low lubricity of hydrogen, which causes premature wear of cooperating elements, such as intake valves and adhesion of engine valve seats, injector needles and their seats (loss of tightness). The second is related to the differently progressing processes of loss of lubricity of the lubricating oil in a hydrogen-powered engine. In this case, the lubricating oil is rapidly diluted with a large amount of water entering it as a result of the hydrogen combustion process. This results in a rapid decrease in the kinematic viscosity of the lubricating oil during operation and the depletion of the potential of anti-seizure and lubricity additives, resulting in a rapid loss of lubricating properties of the oil. This results in significantly shorter drain intervals. In addition, the short hydrogen extinguishing distance results in increased evaporation of the lubricating oil from the cylinder walls and the formation of solid particles (Falfari et al., 2023).

Syed et al. (2019) have shown that many control techniques are being developed to meet the requirements of modern emission standards. The available strategies for controlling NO_x emissions were divided into pre-collection, in-cylinder and post-afterburning techniques. Pre-intake control strategies were assessed to analyse inlet temperature, inlet pressure, flue gas recirculation, O₂ concentration, air/fuel ratio, inert gas addition, water and vapor injection. Control strategies in the cylinder, such as changing the compression ratio, turbulence and injection timing are studied. Various post-afterburning control strategies such as SCR, urea injection, vanadium sublimation, hydrocarbon SCR are explained.

To correctly design a hydrogen-powered engine, it is necessary to adopt a methodology based on both experimental studies and CFD simulations. In addition to LFS estimation, IDT trend prediction is necessary to model the possible self-ignition of the air-hydrogen mixture under the high thermal loads typical of these engines, under stoichiometric or near-stoichiometric conditions. There is little experimental data on air-hydrogen mixtures, especially under engine-like conditions, and it is very difficult to develop a correlation.

Lešnik et al. (2020) concluded that it is important to invest in the development of internal combustion engines for road applications because, despite all the progress, the current road transport system is still based on internal combustion engines and the combustion of petroleum-based liquid fuels. Global demand for petroleum fuels is growing year by year. The total wind and solar power produced in 2016 was able to cover 12 days of the world's energy demand in the transport sector. This shows the dimension of energy demand in the transport sector and points to the complexity of replacing the current energy source. The use of biofuels in combination with modern combustion technologies or hybrid powertrains can have an even greater impact on reducing emissions than any individual solution.

In addition, hydrogen-powered reciprocating combustion engines can be integrated with electric motors in hybrid powertrains. In addition to the efficiency and range benefits, this leads to attractive functional synergies and additional degrees of freedom in terms of design and operation strategies, which need to be taken into account.

5. Hydrogen as an opportunity to meet challenges

The goal of the Paris Agreement is to keep the increase in the global average temperature below 2°C compared to the pre-industrial levels, and to strive to make it no more than 1.5°C. The goal of the European Green Deal is to achieve climate neutrality by 2050. Achieving these targets will require large-scale changes in the transport sector, which is responsible for about a quarter of greenhouse gas emissions. To achieve climate neutrality, it will be necessary to reduce greenhouse gas emissions from transport by 90%. The Earth's population is constantly growing, which translates into a high demand for transportation, which is a major factor influencing the trends in greenhouse gas emissions from vehicles, and mobility patterns are at different stages of development around the world. Today, there are about 1 billion 475 million cars and more than 8 billion people on our globe. It is estimated that the world's population could grow to as high as 11 billion.

One factor that seems to be contributing to limiting the increase in CO₂ emissions is the wider use of biomass fuels, which are considered CO₂ neutral in the emission inventory. However, the raw material used to produce biofuels is decisive as it can negatively affect the reduction of emissions and thus affect the use of biofuels as a solution. For example, indirect land-use change, which can result from the cultivation of crops for biofuels, has the potential to reduce emissions.

In the coming decades, more zero-emission vehicles will be on the road, and existing vehicles will need to become more carbon-intensive and energy-efficient. In order to reduce greenhouse gas emissions and meet the targets, vehicles will increasingly be powered by alternative energy sources in the future. More vehicles will be powered by electric batteries or fuel cells (hydrogen) (see Figure 2). After electrification technology, hydrogen and hydrogen technologies seem to be the most effective.



Figure 2. Transport efficiency based on different power sources in terms of pollutant emissions based on Transport and Environmental based on World bank, National Research Council, Ricardo Energy and Environment, Umweltbundesamt, Apostolaki-losifidou et al., Peters et al., Larmanie et al., Delgado et al. (T&E 2020).

Advances in transport are one of the first steps towards a hydrogen economy. Hydrogen is an energy carrier typically produced from fossil fuels that emit large amounts of CO₂, and the main challenge is to reduce its carbon footprint. If hydrogen is produced by electrolysis using renewable or nuclear energy, the lifecycle greenhouse gas emissions of a vehicle sold in 2024 will be reduced by a factor of 6 compared to diesel. Thus, the decarbonisation of hydrogen production is a prerequisite for ensuring significant climate benefits from the development of hydrogen in transport. From an ecological point of view, compared to battery-powered electric vehicles, the main advantage of hydrogen is the lower battery capacity required. This reduces the pressure on resources and pollution caused by the exploitation of lithium, cobalt or nickel. The hydrogen sector also involves the consumption of metals, in particular platinum for fuel cells and electrolysers. The higher demand for electricity in hydrogen vehicles (produced by electrolysis) requires more metals to produce electricity.

Also, the low volumetric energy density of hydrogen (the amount of energy contained in a given volume) means that its production should take place as close as possible to the point of consumption, to reduce the energy-related and financial costs of transport. This requires considering the organization of ecosystems that allow production and use to be shared between several modes of transport or economic sectors in the same place. To ensure the overall coherence of these regional plans, it will also be necessary to ensure a progressive network of infrastructure for the production and distribution of hydrogen for heavy-duty road transport.

Hydrogen-powered combustion engines are already being used, especially in heavy-duty commercial vehicles. It is a bridging technology to achieve future climate targets for CO₂ emissions and a technology that is more in line with existing automotive knowledge and production. In September 2022, Kawasaki unveiled a hydrogen internal combustion engine developed using the same injector as the one used in the hydrogen Corolla, based on the Ninja H2. In May 2023, Yamaha, Honda, Kawasaki and Suzuki received approval from Japan's Ministry of Economy, Trade and Industry (METI) to form a technological research association called HySE (Hydrogen Small Mobility & Engine Technology) to develop hydrogen-powered engines for small mobility vehicles. The German Association of Technical Inspection (TÜV), which brings together independent service companies from Austria and Germany, intends to promote the conversion of conventionally powered cars to hydrogen. In their opinion, this technology could be a transitional solution on the way to decarbonising transport in line with the goals of climate neutrality, which is going to be cheaper than buying a hydrogen car, especially in transport companies that are not able to replace vehicles with new ones as soon as the objectives of the European Union's climate policy would require. The Fit for 55 proposal provides for the phasing out of internal combustion engines in 2035.

Conclusions

Hydrogen internal combustion engine technology (HICE) builds on the existing internal combustion engines allowing vehicles to be powered by hydrogen. It may be an interim measure until fuel cell technology is further developed. Internal combustion engines have been widely used for decades and are supported by an extensive service network; durable engines that can operate in harsh environments or be subjected to strong vibrations are available in all sizes and configurations.

FCEVs and hydrogen ICE vehicles are not in competition with each other. The development of one technology supports and complements the development of the other as both solutions drive the development of a common infrastructure for hydrogen production, transport and distribution. Also, both solutions involve the same hydrogen storage tanks for vehicles. They are complementary technologies that are currently contributing to the reduction of greenhouse gas emissions generated by vehicles and means of transport and thus working towards the goal of zero emissions.

The processes taking place in the changes in the power source of motor vehicles are inevitable, but they must be evolutionary in character and preceded by numerous studies and tests.

References

Agardy, F.J., Nemerow, N.L. (2005). *Environmental Solutions*. Academic Press. DOI: https://doi.org/10.1016/B978-0-12-088441-4.X5000-X.

Bai-gang, S., Hua-yu, T., Fu-shui, L. (2014). The distinctive characteristics of combustion duration in hydrogen internal combustion engine. *International Journal of Hydrogen Energy*, 39, 14472-14478. DOI: https://doi.org/10.1016/J.IJHYDENE.2014.04.013.

Barbira, F., Basile, A., Veziroğlu, N.T. (2016). *Compendium of Hydrogen Energy: Hydrogen Energy Conversion* (vol. III). Woodhead Publishing Series in Energy. DOI: https://doi.org/10.1016/C2014-0-02674-3.

- Beauregard, G.P. (2011). Findings of Hydrogen Internal Combustion Engine Durability Final Technical/Scientific Report Project Period: 3/7/07–12/31/2010 DE-FC26-06NT43027 Electric Transportation Engineering Corporation 430 S. 2nd Ave Phoenix, AZ 85003.
- Burchart-Korol, D. (2017). Zastosowanie metod oceny środowiskowej na podstawie analizy cyklu życia dla branży motoryzacyjnej. *Zeszyty Naukowe Politechniki Śląskiej. Organizacja i zarządzanie, 100*, nr kol. 1972.
- Centrum Analiz Klimatyczno-Energetycznych. (2022). *Polska netto-zero 2050: rola transportu publicznego w kontekście pakietu "Fit for 55" do 2050*, streszczenie w języku angielskim. Pobrane z: https://climatecake.ios.edu.pl/wp-content/uploads/2022/06/CAKE_Public-trans port-in-PL_2050_Summary_EN.pdf.
- Deloitte. (2018). Zamknięty obieg otwarte możliwości, perspektywy rozwoju gospodarki o obiegu zamkniętym w Polsce. Pobrane z: https://www2.deloitte.com/pl/pl/pages/zarzadzania-procesami-i-strategiczne/articles/innowacje/raport-zamkniety-obieg-otwarte -mozliwosci.html.
- Dimitriou, P., Tsujimura, T. (2017). A review of hydrogen as a compression ignition engine fuel. *International Journal of Hydrogen Energy*, 42, 24470-24486. DOI: https://doi.org/10.1016/J.IJHYDENE.2017.07.232.
- Du, Y., Yu, X., Liu, L., Li, R., Zuo, X., Sun, Y. (2017). Effect of addition of hydrogen and exhaust gas recirculation on characteristics of hydrogen gasoline engine. *International Journal of Hydrogen Energy*, 42, 82888298. DOI: https://doi.org/10.1016J.IJHYDENE. 2017.02.197.
- Duan, J., Liu, F., Sun, B. (2014). Backfire control and power enhancement of a hydrogen internal combustion engine. *International Journal of Hydrogen Energy*, *39*, 4581-4589. DOI: https://doi.org/10.1016/J.IJHYDENE.2013.12.175.
- Edwards, R. (2011). Well-to-Wheels analysis of future automotive fuels and powertrains in the European context. An Commission Joint Research Centre, Institute for Energy WELL-to-WHEELS Report Version 3c, July2011.
- EEA. (2021a). *Emisje gazów cieplarnianych z transportu w Europie, wskaźnik EEA*. Pobrane z: https://www.eea.europa.eu/ims/greenhouse-gas-emissions-from-transpor.
- EEA. (2021b). *Rail and waterborne best for low carbon motorized transport, briefing EEA.* Pobrane z: https://www.eea.europa.eu/publications/rail-and-waterborne-transport.
- EEA. (2021c). *Monitorowanie emisji CO₂ z pojazdów ciężkich, dane EEA*. Pobrane z: https://www.eea.europa.eu/data-and-maps/data/co2-emission-hdv.
- EEA. (2022a). Krajowe emisje zgłaszane do UNFCCC i unijnego mechanizmu monitorowania gazów cieplarnianych, dane EEA. Pobrane z: https://www.eea.europa.eu/data-and-maps/data/national-emissions-reported-to-the-unfccc-and-the-eu-greenhouse-gas-monitoring-mechanism-18.
- EEA. (2022b). Sprawozdanie dotyczące transportu i środowiska 2021. Dekarbonizacja transportu drogowego rola pojazdów, paliwa i zapotrzebowania na transport. Raport EEA nr 2/2022. Pobrane z: https://www.eea.europa.eu/publications/transport-and-env ironment -report-2021.
- Falfari, S., Cazzoli, G., Mariani, V., Bianchi, G.M. (2023). Hydrogen Application as a Fuel in Internal Combustion Engines. *Energies*, 16(6), 2545. DOI: https://doi.org/10.3390/en 16062545.
- FAO. Food and Agriculture Organization of the United Nations. Rome. 2022. The State of the World's Land and Water. Resources for Food and Agriculture 2021 Systems at breaking point. DOI: https://doi.org/10.4060/cb9910en.
- Fennell, D., Herreros, J., Tsolakis, A. (2014). Improving gasoline direct injection (GDI) engine efficiency and emissions with hydrogen from exhaust gas fuel reforming. *International Journal of Hydrogen Energy*, 39, 5153-5162. DOI: https://doi.org/10.1016/J.IJHYD ENE.2014.01.065.
- Ganesan, V. (2012). *Internal combustion engines*. New Delhi, India: McGraw Hill Education (India) Pvt Ltd.

- Gis, M. (2018). *Emisja dwutlenku węgla z transportu drogowego cz. 2 samochody klasy HDV*. Instytut Transportu Samochodowego. Transport Samochodowy 1-2018.
- Goedkoop, M., Spriensma, R. (2001). The Eco-indicator 99. A damage oriented method for Life Cycle Impact Assessment. Methodology. Report. Pre Consultants.
- Gomes Antunes, J.M., Mikalsen, R. Roskilly, A.P. (2009). An experimental study of a direct injection compression ignition hydrogen engine. *International Journal of Hydrogen Energy*, 34, 6516-6522. DOI: https://doi.org/10.1016/J.IJHYDENE.2009.05.142.
- Gurz, M., Baltacioglu, E., Hames, Y., Kaya, K. (2017). The meeting of hydrogen and automotive: A review. *International Journal of Hydrogen Energy*, *42*, 23334-23346. DOI: https://doi.org/10.1016/J.IJHYDENE.2017.02.124.
- Hosseini, S.E. Butler, B. (2020). An overview of development and challenges in hydrogen powered vehicles. *International Journal of Green Energy, 17*(1), 13-37. DOI: https://doi.org/10.1080/15435075.2019.1685999.
- IEA. (2020). Perspektywy technologii energetycznych 2020f. IEA. Paryż.
- IEA. International Energy Agency. (2017a). Future of Trucks.
- IEA. International Energy Agency. (2017b). Energy Technology Perspectives. Deloitte Analysis.
- IEA. International Energy Agency. (2020a). CO₂ emission by sector, World 1990-2018.
- IEA. International Energy Agency. (2020b). CO₂ emission 1) industry, 2) transport and 3) heavy duty vehicles in sustainable development scenario 2000-2030. Deloitte Analysis.
- IEA. International Energy Agency. (2020c). Transport sector CO₂ emissions by mode.
- IEA. International Energy Agency. (2020d). Tracking Transport. Deloitte analysis.
- IEA. International Energy Agency. (2020e). Energy Technology Perspectives.
- IEA. International Energy Agency. (2022). Global EV Outlook 2022 Securing supplies for an electric future. Pobrane z: https://iea.blob.core.windows.net/assets/e0d2081d-487d-4818-8c59-69b638969f9e/GlobalElectricVehicleOutlook2022.pdf.
- IEA. International Energy Agency. (2022). Global EV Outlook 2022 Securing supplies for an electric future. Pobrane z: https://iea.blob.core.windows.net/assets/e0d2081d-487d-4818-8c59-69b638969f9e/GlobalElectricVehicleOutlook2022.pdf.
- Jakóbiec, J., Kamiński, A., Pusz, A. (2021). Możliwe kierunki rozwoju przemysłu rafineryjnego w Polsce. *Przemysł Chemiczny*, *11*, 997-1002. DOI: https://doi.org/10.15199/62.2021.11.1.
- Juste, G.L., Benavides, E.M. (2008). Feasibility analysis of hydrogen as additional fuel in aircraft propulsion. *International Journal of Green Energy*, 5, 69-86. DOI: 10.1080/15435070701839421.
- Kamiński, A. (2014). Zmiany w prawie europejskim implikujące zmiany w sposobie wytwarzania, składzie chemicznym i dystrybucji paliw. *Studia Ecologiae et Bioethicae UKSW*, 12(3), 163-187.
- Kamiński, A. (2015). Krajowe i ogólnoświatowe wymagania środowiskowe w aspekcie jakości paliw. *Studia Ecologiae et Bioethicae, UKSW, 13*(1), 163-187.
- Kamiński, A., Jakóbiec, J., Pusz, A. (2021). Sources of Emissions in Refinery Legal Regulations and Costs. *Journal of Ecological Engineering, Polish Society of Ecological Engineering (PTIE)*, 22(11), 53-61. DOI: https://doi.org/10.12911/22998993/142973.
- Kamiński, A., Pusz, A., Drewniak, Ł. (2018a). Określenie stanu gleby na terenie stacji dystrybucji paliw dla jej potencjalnej remediacji. *Przemysł Chemiczny*, 97(3), 410-415. DOI: https://doi.org/10.15199/62.2018.3.13.
- Kamiński, A., Pusz, A., Drewniak, Ł. (2018b). Remediacja środowiska gruntowo-wodnego na terenie stacji dystrybucji paliw metodą in situ. *Przemysł Chemiczny, 97*(9), 1575-1579. DOI: https://doi.org/10.15199/62.2018.9.38.
- Kamiński, A., Pusz, A., Wiśniewska, M. (2019). Ocena fitotoksyczności gleb zanieczyszczonych substancjami ropopochodnymi. *Przemysł Chemiczny*, 98(6), 857-862. DOI: https://doi.org/10.15199/62.2019.6.4.

- KE. Komisja Europejska. (2011). Bruksela, dnia 28.3.2011. COM(2011) 144 wersja ostateczna Biała Księga. Plan utworzenia jednolitego europejskiego obszaru transportu dążenie do osiągnięcia konkurencyjnego i zasobooszczędnego systemu transportu.
- KE. Komisja Europejska. (2019). Komunikat Komisji do Parlamentu Europejskiego, Rady Europejskiej, Rady, Komitetu Ekonomiczno-Społecznego i Komitetu Regionów. Europejski Zielony Ład. COM/2019/640 final.
- KE. Komisja Europejska. (2020). Bruksela, dnia 9.12.2020 r. COM(2020) 789 final. Komunikat Komisji do Parlamentu Europejskiego, Rady, Europejskiego Komitetu Ekonomiczno-Społecznego i Komitetu Regionów Strategia na rzecz zrównoważonej i inteligentnej mobilności europejski transport na drodze ku przyszłości {SWD(2020) 331 final}. Pobrane z: https://data.consilium.europa.eu/doc/document/ST-14012-2020-INIT/pl/pdf.
- KE. Komisja Europejska. (2022a). Wydajny, bezpieczny i przyjazny dla środowiska transport. Pobrane z: https://ec.europa.eu/info/strategy/priorities-2019-2024/european-green-deal/transport-and-green-deal_pl.
- KE. Komisja Europejska. (2022b). Dekarbonizacja europejskiego sektora transportu. Pobrane z: https://cordis.europa.eu/article/id/436498-decarbonising-europe-s-transport-sector/pl.
- Keesom, B., Blieszner, J., Unnasch, S. (2012). EU Pathway Study: Life Cycle Assessment of Crude oils in a European Context. Jacobs Consultancy.
- Krajowy Ośrodek Bilansowania i Zliczania Emisji (KOBiZE). (2021). Emisje gazów cieplarnianych i innych zanieczyszczeń w sektorze transportu samochodowego w Polsce uwarunkowania i możliwości redukcji. IV Forum Innowacyjności. Polska droga do czystego transportu.
- Lešnik, L., Kegl, B., Jiménez, E.T., Cruz-Peragón, F. (2020). Why we should invest further in the development of internal combustion engines for road applications. *Oil & Gas Science and Technology Rev. IFP Energies Nouvelles*, 75(56). DOI: https://doi.org/10.2516/ogst/2020051.
- Muhammad Imran Khan. (2018). Comparative Well-to-Tank energy use and greenhouse gas assessment of natural gas as a transportation fuel in Pakistan. *Energy for Sustainable Development*, 43, 38-59.
- Naber, J.D., Siebers, D.L. (1998). Hydrogen combustion under diesel engine conditions. *International Journal of Hydrogen Energy*, 23, 363-371. DOI: https://doi.org/10.1016/S0360-3199(97)00083-9.
- OECD. Organization for Economic CO-Operation and Development. (2019). *ITF Transport Outlook*. Pobrane z: https://www.oecd-ilibrary.org/transport/itf-transport-outlook-2019_transp_outlook-en-2019-en.
- Onorati, A., Payri, R., Vaglieco, B.M., Agarwal, A.K., Bae, C., Bruneaux, G., Canakci, M., Gavaises, M., Günthner, M., Hasse, C., Kokjohn, S., Kong, S.C., Moriyoshi, Y., Novella, R., Pesyridis, A., Reitz, R., Ryan, T., Wagner, R., Zhao, H. (2022). The role of hydrogen for future internal combustion engines. *International Journal of Engine Research*, 23(4), 529-540. DOI: https://doi.org/10.1177/14680874221081947.
- Organization for Economic CO-Operation and Development (OECD). (2020). *Road Freight Transport TKM*. Pobrane z: https://data.oecd.org/transport/freight-transport.htm.
- Parlament Europejski. (2022). *Emisje CO₂ z samochodów: fakty i liczby (infografiki)*. Pobrane z: https://www.europarl.europa.eu/news/pl/headlines/society/20190313STO31218/emisje-co2-z-samochodow-fakty-i-liczby-infografiki.
- Peschka, W. (1998). Hydrogen: The future cryofuel in internal combustion engines. *International Journal of Hydrogen Energy*, 23, 27-43. DOI: https://doi.org/10.1016/S0360-3199(97)00015-3.
- Pusz, A., Kamiński, A. (2023). Analiza kosztów i korzyści wariantów remediacji historycznych zanieczyszczeń powierzchni ziemi stwierdzonych na terenie obiektu dystrybucji paliw. *Przemysł Chemiczny, 12*, 154-160. DOI: https://doi.org/10.15199/62.2023.12.19.
- Rezaei, R., Sens, M., Riess, M., Bertram, C. (2021). Potentials and challenges of hydrogen combustion system development as a sustainable fuel for commercial vehicles. In: *Internationaler Motorenkongress* 2021. PROCEE (pp. 99-114). Conference paper. DOI: 10.1007/978-3-658-35588-3

- Rogowska, D., Jakóbiec, J. (2014). Emisja GHG w cyklu życia paliw silnikowych. Część I wytyczne do konstruowania bilansu masowego produkcji. *Nafta-Gaz*, *LXX*(9).
- Scott, J., Curran, R.M., Wagner, Ronald, L., Graves, M., Keller, Johney, B., Green Jr. (2014). Well-to-wheel analysis of direct and indirect use of natural gas in passenger vehicles. *Energy*, 75, 194-203. Pobrane z: www.elsevier.com/locate/energy.
- Sen, A., Miller, J. (2022). *Emissions reduction benefits of a faster, global transition to zero-emission vehicles*. Working Paper 2022-15. ICCT International Council on Clean Transportation. Pobrane z: https://theicct.org/wp-content/uploads/2022/03/Accelerated-ZEV-transition-wp-final.pdf.
- Sopena, C., Diéguez, P.M., Sáinz, D., Urroz, J. C., Guelbenzu, E., Gandía, L.M. (2010). Conversion of a commercial spark ignition engine to run on hydrogen: Performance comparison using hydrogen and gasoline. *International Journal of Hydrogen Energy, 35*, 1420-1429. DOI: https://doi.org/10.1016/J.IJHYDENE.2009.11.090.
- Sosa, Y. (2022). *Hydrogen-powered vehicles: Is the third time the charm? Tribology and Lubrication Technology*. (TLT) Society of Tribologists and Lubrication Engineers.
- Stepień, Z. (2021). Kompleksowy przegląd silników spalinowych napędzanych wodorem: osiągnięcia i przyszłe wyzwania. *Energies*, *14*(20), 6504. DOI: https://doi.org/10.3390/en14206504.
- Stępień, Z. (2023). Analysis of the prospects for hydrogen-fuelled internal combustion engines Combustion Engines. DOI: https://doi.org/10.19206/CE-174794.
- Stępień, Z. (2023). Fuels of the future challenges for lubricants. XIII Międzynarodowa Konferencja Naukowo-Techniczna Środki Smarowe 2023, Starachowice, 23-25 października 2023 r.
- Stępień, Z., Urzędowska, W. (2021). Tłokowe silniki spalinowe zasilane wodorem wyzwania. *Nafta-Gaz, 12*, 830-840. DOI: https://doi.org/10.18668/NG.2021.12.06.
- Stępień, Z. (2023). Synthetic Automotive Fuels. *Combustion Engines*, 192(1), 78-90. DOI: https://doi.org/10.19206/CE-152526.
- Syed, S., Renganathan, M. (2019). *NO_x emission control strategies in hydrogen fuelled automobile engines*. DOI: https://doi.org/10.1080/14484846.2019.1668214.
- Szwaja, S., Grab-Rogaliński, K. (2009). Hydrogen combustion in a compression ignition diesel engine. *International Journal of Hydrogen Energy, 34*, 4413-4421. DOI: https://doi.org/10.1016/J.IJHYDENE.2009.03.020.
- T&E. (Transport and Environment). (2020). *Decarbonising the EU's transport sector with renewable electricity and electrofuels*. Pobrane z: https://www.transportenvironment. org/wp-content/uploads/2020/12/2020_12_Briefing_feasibility_study_renewables_deca rbonisation.pdf.
- Tartakovsky, L., Sheintuch, M. (2018). Fuel reforming in internal combustion engines. *Progress in Energy and Combustion Science*, 67, 88-114. DOI: https://doi.org/10.1016/J.PECS. 2018.02.003.
- Umweltbundesamt. (2022). *Klimaschutz im Verkehr*. Pobrane z: https://www.umweltbundesamt.de/themen/verkehr-laerm/klimaschutz-im-verkehr#undefiniowane.
- Verhelst, S., Sierens, R. (2001). Hydrogen engine-specific properties. *International Journal of Hydrogen Energy*, 26, 987-990. DOI: https://doi.org/10.1016/S0360-3199(01)00026-X.
- Wang, L., Yang, Z., Huang, Y., Liu, D., Duan, J., Guo, S., Qin, Z. (2017). The effect of hydrogen injection parameters on the quality of hydrogen—Air mixture formation for a PFI hydrogen internal combustion engine. *International Journal of Hydrogen Energy, 42*, 23832-23845. DOI: https://doi.org/10.1016/J.IJHYDENE.2017.04.086.
- WCED. World Commission on Environment and Development. (1991). *Nasza wspólna przyszłość:* raport Światowej Komisji do spraw Środowiska i Rozwoju. Państwowe Wydawnictwo Ekonomiczne.

DESTRUCTION OF FUNCTIONAL SYSTEMS OF A DIESEL ENGINE RESULTING FROM THE FORMATION OF PM DEPOSITS

Bogusław Cieślikowski¹

¹ University of Applied Sciences in Nowy Sącz, Faculty of Engineering Sciences, Zamenhofa 1A, 33-300 Nowy Sącz, Poland; e-mail: bcieslikowski@ans-ns.edu.pl

Abstract: Optimization of the fuel combustion process in a diesel engine with multi-stage HPCRS (High Pressure Common Rail System) injection sets the main directions of research in the field of thermodynamic stability of fuels with the addition of FAME, including the processes of PM (Particulate Matter) formation. These particles absorb heavy metals, sulfur and nitrogen compounds, and PAH hydrocarbons (Polycyclic Aromatic Hydrocarbons), which may include directly or indirectly carcinogenic substances. It is necessary to precisely control the recirculated exhaust gas stream to achieve the desired NOx emission reduction effects. The diagnostic procedure of the 2.0 dCi M9R engine showed the formation of PM deposits in both the EGR (Exhaust Gas Recirculation) and DPF (Diesel Particulate Filter) systems, which requires the use of interdependent OBDII (On-Board Diagnostic level 2) diagnostic tests. An ineffective effect of the DEF filter regeneration process and error codes DF315 and DF890 were recorded, as well as an incorrect value of the recirculation degree. XEGR, leading to signaling of the engine operating status via the MIL (Malfunction Indicator Light) and also recording error codes DF647 and DF647. Analyses of the XRF spectrum of sediments forming PM together with the IR spectrum of infrared spectroscopy showed the participation of organic compounds of FAME origin.

Keywords: EGR (Exhaust Gas Recirculation), DPF (Diesel Particulate Filter), FAME (Fatty Acid Methyl Esters) biofuel, OBD II diagnostics (On-Board Diagnostic level 2.).

Introduction

The chemical formula of motor fuels is constantly evolving due to the requirements for improving combustion processes, the technical condition of engine components, environmental protection and the development of the design of drive units (Caprotti et al., 2005; CEC/TC 19 WG24, 2011). Optimization of the combustion process in a diesel engine with the multi-stage injection of a hydrocarbon fuel with the addition of biocomponents determines the main directions of research in the field of thermodynamic stability of fuels and the development of engine designs equipped with the HPCRS (High Pressure Common Rail System) (Quigley et al., 2009). Oxidation resistance is one of the most important properties of fuel containing FAME components (Fatty Acid Methyl Esters) due to their low stability, resulting in the formation of products that threaten the proper functioning of the engine (Stanik et al., 2013).

The progressive improvement of the physicochemical parameters of fuel with the addition of biocomponents requires specialized research to identify functional features and indicate possible solutions. Some properties of biocomponents, such as high viscosity, low volatility, olefin content and aromatic compounds, facilitate the formation of PM carbon deposits in the injector hole zone, combustion chamber, turbocharger, DPF and EGR systems (Pehan et al., 2009). The gradual increase in PM deposits leads to the loss of the ability to properly atomize the fuel, immobilization of the VTG (Variable Turbine Geometry) compressor exhaust vane positioning mechanism, blockage of the EGR valve and a decrease in the throughput of the DPF filter (Cieślikowski, 2011).

This process leads to the occurrence of engine failure states related to the recording of error codes in the ECU (Engine Control Unit or ECM Engine Control Module), signaling of the MIL indicator and switching to the substitute operating characteristics of the engine (Gunter, 2010). The complex nature of recording error codes requires a multi-aspect diagnostic inference process, also analysing the recording of engine operating parameters as dynamic characteristics in a parallel system in the time base of the test being created (Cieślikowski, Jakóbiec, 2018).

1. Causes of IDID (Internal Diesel Injector Deposits) formation

The FAME contained in diesel oil additionally promotes the formation of IDID (Internal Diesel Injector Deposits) deposits through acidic impurities generated during the production of FAME, formed in the autocatalytic division of fatty esters with the participation of metal ions. PIBSI (Polyisobutylene bis Succinic Anhydride) with a high amine content in interaction with carboxylic dimers of fatty acids are particularly susceptible to the formation of these deposits (Stanik et al., 2015). The resulting deposits are insoluble in basic organic solvents, which makes their analysis and determination of their chemical structure very difficult. The deposits created in this way may cause the surfaces of interacting elements to stick together and intensify corrosion processes (Merkisz, Mazurek, 2007).

Previous research also indicates the possibility of IDID formation from fuel oxidation products, especially in the case of unstable diesel fuels containing FAME, or may come from the aging of higher fatty acid esters found in lubricant additives (Novel-Cattin et al., 2000). Multifunctional detergent-dispersant packages for diesel fuels require compatibility and stability tests, as they consist of many different additives and may interact and show incompatibility, leading to turbidity, delamination and the formation of deposits (Pehan et al., 2009).

Progress in the technology of detergent-dispersant additives and their dosing level allows to solve many of the above problems. A multifunctional detergent-dispersant package for technologically advanced diesel fuels must perform many functions to protect high-pressure HPCRS systems against internal IDID deposits, coking of nozzles, wear and seizure of the high-pressure fuel pump and corrosion of the fuel system. Moreover, it should protect diesel fuel against oxidation, having the ability to wet metal surfaces and create a protective film that prevents the deposition of highly adhesive deposits and varnishes, thus keeping multi-hole injectors clean (Cieślikowski, 2018).

2. Functional analysis of engine components subject to OBD II control

The fundamental problem of assessing the correct operation of the EGR valve results from the inability to read the position of the valve controlling the return flow of exhaust gases in the online system, because the time histories of the valve stepper motor control signals are not recorded. Few diagnostic testers only allow reading the

average value of the EGR valve positioning, because the data of each stepper motor excitation against the background of changes in other operating parameters of the combustion engine are not recorded. The positioning of the EGR valve is controlled by a stepper motor, usually consisting of two pairs of windings, using an alternating key-switch, ensuring a change in the angle and direction of rotation as a result of a sequence of pulses generated by digital or microprocessor systems. These systems are protected against overvoltages due to the high self-induction voltage generated.

The modulation of the EGR valve opening determines the mass of the exhaust gas flow to provide an instantaneous value of the recirculation rate. XEGR. The degree of recirculation X_E for the instantaneous throughput value of the EGR valve is determined by the ratio of the mass of exhaust gases directed through the EGR valve, m_E [kgs⁻¹], to the sum of the mass of air $m_p[kgs^{-1}]$ and $m_E[kgs^{-1}]$. The error range is strictly defined and exceeding this value determines an emission fault, leading to the signaling of the MIL indicator for an engine emergency condition. Identification of EGR valve positioning errors is a complex procedure because a group of mutually coupled signals coming from the stepper motor of the exhaust gas flow control valve actuator is analysed concerning to the signal from the mass air flow meter, the pressure in the intake system MAP (Manifold Absolute Pressure Sensor), representative sensors temperatures, shaft speed and systems causing changes in valve timing. It is necessary to ensure the required stoichiometry of the total mass of the charge sucked into the cylinder, which is a mixture of air and exhaust gases with variable proportions and is calculated by the ECU controller based on parameters such as: shaft rotation speed, the mass of intake air, boost pressure, and temperature of the components. A significant simplification is usually used to determine the mass of recirculated exhaust gases, determined from the difference between the total mass of the charge and the mass of air concerning to the temperature correction of the intake air, and comparing this value in the existing engine loads with the value stored in the controller's memory.

Therefore, the indicated approximations of the actual state of the control object indicate a high degree of functional imperfection of the analysed system. The situation is aggravated by the inability to take into account variable exhaust gas flow resistance in the zone of the valve controlling the flow of recirculated exhaust gases due to PM carbon deposits, as well as the variability of exhaust gas composition depending on the share of biocomponents in diesel oil (Eastwood, 2020).

The EGR valve diagnostics process, which consists solely of reading fault codes stored in the ECU controller memory, should be supplemented with the reading of actual parameters and extended analysis of voltage signals using an oscilloscope. The lack of direct measurement of the mass flow rate of recirculated exhaust gases at variable temperature of the medium at the cylinder inlet should be taken into account.

Therefore, the momentary measurement of the mass of air sucked in by the engine is reduced by the mass of supplied exhaust gases, which modulates the momentary values of the voltage signals of the air flow meter, generating a signal enabling the analysis of the degree of these changes depending on the engine load. Therefore, the signal from the intake air mass sensor can be extended with oscilloscope diagnostics, providing the basis for assessing the correctness of the transmitted signal of variability of the exhaust gas recirculation degree. Disturbances in this measurement may result

from the averaging of the medium flow conditions with variable channel geometry in zones with different wall temperatures, which is also due to the accumulation of PM deposits. The formation of deposits in the intake manifold and head channels may also be the result of improper venting of the engine crankcase with floating particles of lubricating oil, which is usually associated with excessive blow-by of exhaust gases and malfunction of the oil separator as well as wear of the turbocharger bearings, causing oil particles to enter the manifold suction. The situation is aggravated by the gradual deterioration of the lubricating parameters of engine oil as a result of failure to comply with oil and filter replacement deadlines as well as the use of substitutes of inadequate quality.

These factors also influence the progressive decline in the DPF filter cleaning efficiency, with the display of an increasing LED line in the central cockpit display unit or only the filter filling limit symbol (approx. 70-80%). There is no information about the impossibility of active filter regeneration due to the inappropriate vehicle traction process, or a warning about the borderline filling of the filter channels with unremovable ash (Wiedemann, Neumann, 1995).

Overfilling the DPF with ash, which is not removed during the filter regeneration process, results in frequent attempts by the ECU controller to initiate the active regeneration procedure. This process contributes to the penetration of excess unburnt fuel into the engine crankcase and leads to the destruction of engine oil. Important symptoms of this condition, apart from the error codes saved in the controller: P2452 (DPF pressure sensor circuit), P2453 (DPF pressure sensor circuit range) and the MIL warning light, are a drop in engine power as a result of the ECU switching to emergency mode and an increase in the value of instantaneous fuel consumption signaled on the MFA (Multifunktionsanzeige) or FIS (Fahrer Information System) display.

The limit value of flow resistance through the DPF is usually determined by a pressure difference of approximately 200 mbar. There have been cases of damage to the DPF differential pressure sensor as a result of a decrease in the tightness of the flexible pipes or their lack of patency due to PM retention. The correct operation of the differential pressure sensor should be checked using a pressure gauge, setting the pressure at the connection indicated by the factory data for the zone before and after the filter and observing the limit voltage readings (approx. 0.8 V) for a reference voltage of 5V and modulation from 0.5 to 4.5V for the signal cable. The classic method of DPF regeneration is the combustion of organic products contained in PM (mainly soot and hydrocarbons), and the process activation energy for after-combustion of PM generated from diesel oil is from 160 to 172 kJ/mol, which corresponds to temperatures of 420-600°C.

Therefore, active regeneration requires, in addition to the DPF differential pressure monitoring system, modification of the HCPR system operating mode to provide the necessary energy to initiate the process. Regeneration is supported by covering the walls of the filter monolith with a layer of platinum catalyst, which allows the soot oxidation temperature to be reduced to approximately 440-460°C. The use of FBC (Fuel Borne Catalyst) fuel additives can reduce the activation temperature of the process even to approximately 300-350°C (Campenon et al., 2004).

The process occurring during equilibrium DPF regeneration is a chain reaction operating according to the free radical mechanism. The kinetic equation of the transformation at a constant reaction rate depending on the temperature, which can be described by the Arrhenius equation describing the principle: the lower the activation energy, the higher the reaction rate (Mayer et al., 1980):

$$k = Ae^{-E/RT}$$

where:

k – reaction rate constant,

A – characteristic constant of the reaction,

 $R - universal gas constant 8,31446261815324(J/mol^{-1} K^{-1}),$

E – activation energy (J/mol⁻¹).

The process initiating regeneration is the ignition of hydrocarbons on the PM surface, which causes a local temperature increase. The increase in the share of biocomponents in hydrocarbon fuel and sediments from the soluble organic fraction SOF (Soluble Organic Fraction) will limit the rapid burning of the entire PM mass accumulated in the DPF, which contributes to reducing the risk of DPF filter destruction. Moreover, the value of hydrocarbon concentration with a variable share of higher fatty acid methyl esters FAME should be taken into account in the kinetic equation of the reaction. Another major difficulty is determining the specific heat of recirculated exhaust gases based on the specific heat of its individual components and determining their mass fractions.

Excessive mass of PM remaining in the DPF causes increased back pressure in the exhaust gas system and increased exhaust gas recirculation, affecting the interdependent implications of EGR system failure states. As a consequence, PM emissions increase, the oxygen content in exhaust gases decreases, and NOx emissions increase. These factors have an adverse effect on the initiation of DPF regeneration processes, which leads to irreversible processes of blocking the DPF capacity and a rapid deterioration of engine operating parameters. Moreover, the DPF regeneration process causes a sharp increase in HC and CO emissions. Carbon monoxide is the result of the regeneration process reacting too quickly with insufficient oxygen available.

Research and assessment of secondary emission levels are still being carried out both for filtering systems containing catalytically coated monoliths and for systems based on the use of FBC (Fuel Borne Catalyst) additives to fuel to support DPF regeneration processes (Brewbaker, Nieuwstadt, 2002; Wickström, 2012).

3. Object of OBDII diagnostic tests

The object of the research was a 2.0 dCi M9R passenger car engine showing a malfunction indicated by the MIL indicator. Using dedicated testers, diagnostic procedures were carried out, including the assessment of engine operating parameters and analysis of stored error codes according to ISO markings and factory coding. The vehicle tests were carried out using various interfaces in order to compare the quality of the diagnostic process, using a dedicated CAN CLIP 213, KTS 540 scanner from BOSCH, Navigator TXTs TEXA working with the IDC5 CAR PLUS software, which communicated with the vehicle via a 16-pin OBDII socket. An ineffective effect of

the DEF filter regeneration process was demonstrated due to the accumulation of non-removable PM layers, leading to an excess differential pressure value and errors codes DF315 and DF890. Usually, the excess value of sediment mass indicates low DPF regeneration efficiency, which results mainly from the use of the vehicle over short distances.

The DPF regeneration process should take place every few thousand kilometers while maintaining a constant driving speed without changing gear ratios in the drive train, maintaining high engine shaft speeds. In the case of using a car in urban locations, these conditions are difficult to implement. PM deposits made it impossible to obtain the correct DPF throughput rate, which contributed to the inability to ensure the correct value of the X_E exhaust gas recirculation rate, contributing to the failure being recorded as error codes DF647 and DF647. A large oscillation of the exhaust gas recirculation degree value at idle speed results in fluctuations of the engine shaft revolutions and, together with the display of error codes, justifies the indication of the causes of excessive PM retention on the elements throttling the exhaust gas flow. In the analysed case, this parameter ranged from 5 to 29%, with pulsations of the mass air flow measured by the flow meter ranging from 47 to 136 g/s. In addition, the "freeze frame" parameters were read for the purpose of analysing engine operating parameters after detecting errors by the controller. Simplified diagnostic reasoning indicates the need to replace or attempt to clean the EGR valve and DPF filter with chemicals.

However, you should first check the number of kilometers the car has traveled since the state of proper DPF regeneration recorded in the engine ECU. In the analysed case, the exhaust gas temperature sensor before the DPF filter showed readings below 160°C, i.e. below the value of the condition for starting DPF filter regeneration. Incorrect operation of the exhaust gas temperature sensor prevented the filter regeneration process, leading to an excess differential pressure value and the error code DTC 203115.

After replacing the temperature sensor, the engine was tested again, ensuring the previously required traction conditions for DPF regeneration, which, however, showed low effectiveness of DPF regeneration (Table 1). At a differential pressure of 30 mbar, the filter regeneration occurred at a sediment level of 41g, reaching a value after the process completion of approximately 35g, which proves that it is impossible to remove the thermally stabilized sediment layer. After completing the engine tests, the PDF and EGR valve were dismantled to collect samples of PM deposits from the DPF PM inlet zone for spectral analyses (Figure 1).

Table 1
Recording of the functional parameters of the filter pressure

No.	Parametr	Numeric value	Unit of measurement
1.	Mass of sediment in the particulate filter DPF	41	g
2.	Mass of sediment in the particulate filter DPF after regeneration	35	g
3.	Cold engine DPF – deposit mass limit	5	g
4.	1. Number of failed regeneration attempts 5		
5.	5. Number of successful regenerations 2		
6.	Temperature before particle filter DPF	160	$^{\circ}\mathrm{C}$
7.	Particulate filter DPF – differential pressure	30	mbar.

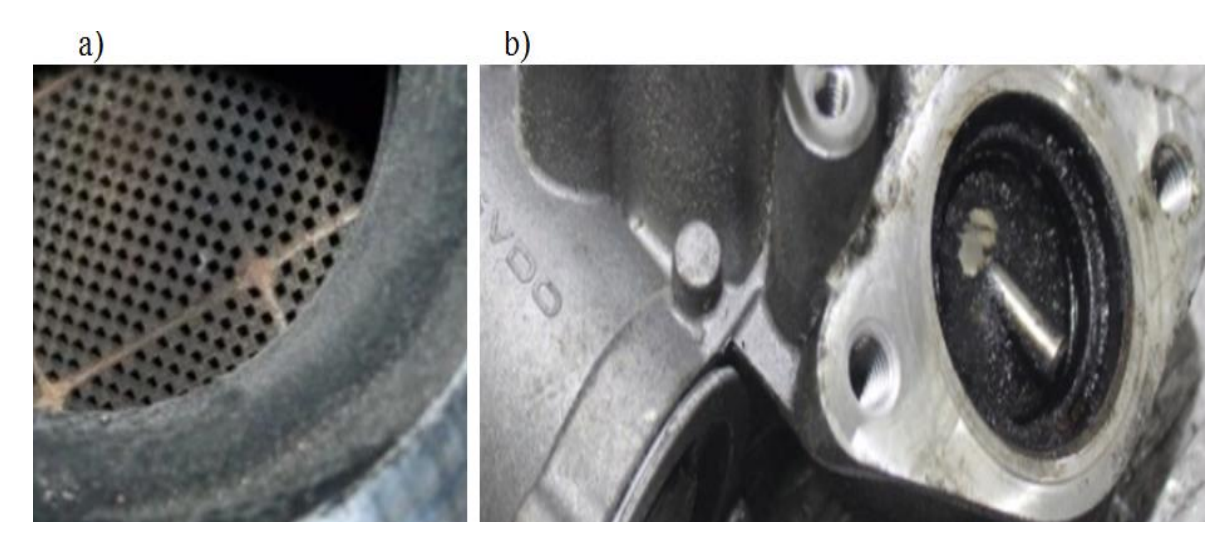


Figure 1. Fragment of the DPF inlet zone (a) and EGR valve (b) from which samples of PM deposits were taken for spectral analyses.

When applying the principles of extended diagnostic reasoning, attention should be paid to the correctness of fuel injection in the HPCRS system, despite the lack of an error code indicating the failure of the fuel injectors. After checking the representative parameters of the system, mainly the correction doses of individual injectors, a large variation in the value of this parameter was found despite the fact that the threshold values were not exceeded and another error code was recorded (Table 2). Noteworthy is the large value of positive fuel dose correction for the 3rd cylinder.

Table 2
Control of correction doses of HPCRS injectors

No.	Parametr	Numeric value	Unit of measurement
1.	Fuel dose correction for the – 1 cylinder	-2,9	mm^3
2.	Fuel dose correction for the – 2 cylinder	-15	mm^3
3.	Fuel dose correction for the – 3 cylinder	3,1	mm^3
4.	Fuel dose correction for the – 4 cylinder	1,3	mm^3

A large positive value of the fuel dose correction is not indifferent to the formation of excess PM deposits in the DPF, EGR valve and exhaust gas cooler, as well as in the VTG turbocharger, consequently leading to blocking of the exhaust gas guide positioning mechanism. The diagnosis result is complemented by demonstrating the correct course of the exhaust gas recirculation degree during the test run at a maximum speed. 110 km h⁻¹ (Figure 2). Analysing the characteristics, it can be concluded that the required boost pressure values (purple line) and measured values (green line) are very similar. The air pressure behind the turbocharger is over 2320 mbar, which in relation to the required value of 2300 mbar is the correct value with a time shift of approximately 0.5 s resulting from the delay in the increase of exhaust gas flow and rotor inertia. It should also be noted that when increasing the driving speed, the recirculation valve remains in the closed position.

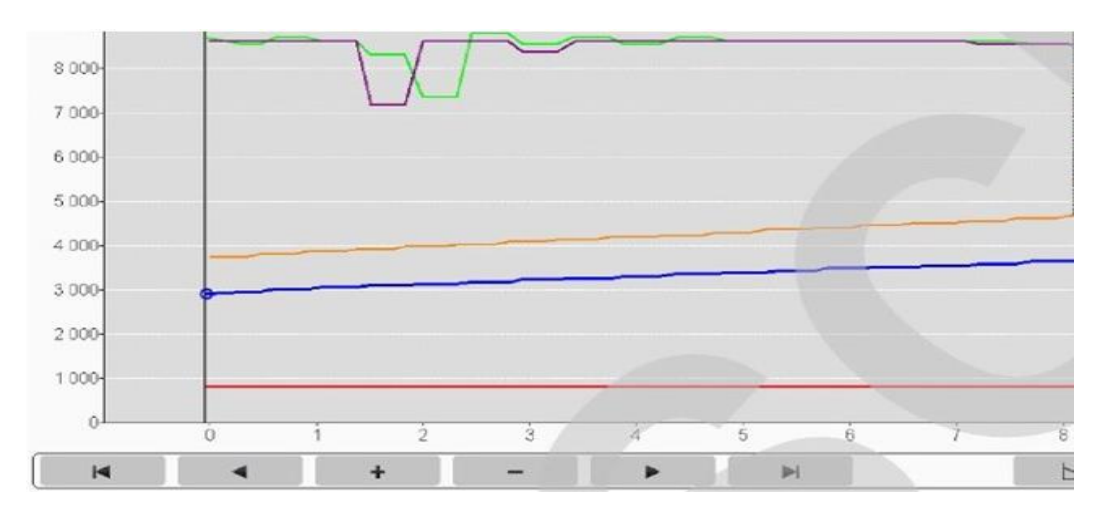


Figure 2. Measurement values related to the required: – measurement of boost pressure (green line) And reference pressure (violet line), – engine speed (max. 2900 min⁻¹), – driving speed (max. 110 km h⁻¹), – positioning of the EGR valve during acceleration (red line).

4. Spectral analyses of PM sediments

A spectral analysis of sediments was carried out to determine the composition of PM collected from the DPF inlet zone and the EGR valve (Sadle, 2002). Microscopic analysis of the sediment revealed sediment grains that were stuck together with a tarry substance. The sediment collected from the area of the DPF inlet channels was characterized by a more fine-grained structure with a fraction of mineral material. Both fuel and engine oil residues and their degradation products were observed. After washing the sediments from the outer surface of the analysed zones with chloroform, the samples were analysed in the infrared spectrum. Infrared IR (FTIR) spectra were recorded on BIO-RAD's FTS 175. The infrared spectra of the soluble part of the sediment originating from the EGR and DPF valve zone are presented in Figure 5, while the analysis of the characteristic bands is presented in Table 3. Analyses of the infrared spectroscopy spectrum showed a significant share of organic compounds of FAME origin in the solid PM sediment.

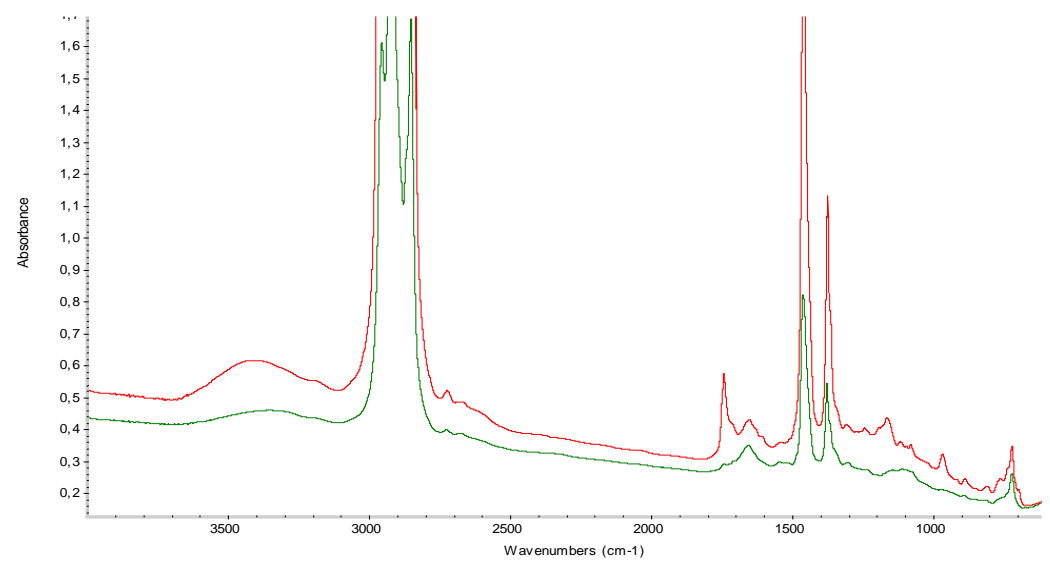


Figure 3. Infrared spectrum of the soluble part of the sediment coming from the EGR valve zone (green) and DPF (red).

Table 3
Analysis of characteristic wavenumber values [cm⁻¹]

- 2	idiysis of characteristic wavenumber values [cm]			
No.	wave number [cm ⁻¹]	Identification	Final results of chemical and thermodynamic processes	
1.	722	hydrocarbon groups	raising the background, which is related to the presence of PM	
2.	1377	hydrocarbon groups	engine oil derivatives and their degradation products	
3.	1464	hydrocarbon groups	raising the context of the relationship with the occurrence of PM	
4.	1630	derivatives of compounds containing bonds C-O-NO ₂	the result of nitrooxidation of engine oil and fuel components in contact with nitrogen oxides	
5.	1655	oxidation processes of organic compounds	high band intensity – the result of oxidation processes of organic compounds to carbonyl and carboxyl structures	
6.	1747	presence of esters	relationships of carbonyl groups C=O (aliphatic) with the band in the area of 1750-1735 cm ⁻¹	
7.	2000-1600	oxidation processes of organic compounds	occurrence of oxidation processes of organic compounds to carbonyl and carboxyl structures	
8.	2850-3000	hydrocarbon groups	high band intensity – strong background elevation, which is related to the presence of PM along with engine oil degradation products	
9.	ok. 3400	hydroxyl groups	The effect of water sorption and also as a derivative of the structures of alcohols and carboxylic acids	

Conclusions

Diagnostic testing procedures using a dedicated tester should strive to fully illustrate the operating parameters of interdependent engine systems and not focus on single symptoms of reduced functionality of the systems or replace components according to the list of error codes. The indications also concern the advisability of using diagnostic inference procedures covering multi-symptom states of engine failure resulting from the synergy of data exchange between engine functional systems using an IT bus. Excessive deposits on the DPF filter structure and elements controlling the exhaust gas flow through the EGR valve may be caused by the increasing fuel dose correction value before it reaches the limit value signaled by the MIL indicator. Only the last step is deleting errors stored in the controller's memory, which should always be performed after repairing or replacing damaged elements. Infrared spectroscopy analyses showed a significant share of organic compounds of FAME origin in the solid PM deposit.

References

- Brewbaker, T., Nieuwstadt, M. (2002). Control of Oxygen for Thermal Management of Diesel Particulate Filters. *SAE Paper 2002-01-0427*.
- Campenon, T., Wouters, P., Blanchard, G., Macaudiere, P., Seguelong, T. (2004). Improvement and Simplification of DPF System Using Ceria-based Fuel-Borne-Catalyst for DPF Regeneration in Serial Applications. *SAE Paper 2004-01-0071*.
- Caprotti, R., Breakspear, A. et al. (2005). Detergency Requirements of Future Diesel Injection System. *SAE Paper 2005-01-3901*.
- CEC/TC 19 WG24: Report of the Ad-hoc Injector Sticking Task Force 02 August 2011.
- Cieślikowski, B. (2011). Spectral analysis of deposits from a catalytic converter of Diesel engine. *Combustion Engines*, *3*(146), 1-6.
- Cieślikowski, B., Jakóbiec, J. (2018). Influence of Internal Deposits on Diesel Engine Injectors on the Parameters of the High Pressure Common Rail System (HPCR). In: *Renewable Energy Sources: Engineering, Technology, Innovation* (pp. 463-472). Springer Proceedings in Energy.
- Eastwood, P. (2000). *Critical Topics in Exhaust Gas Aftertreatment*. Ford Motor Company. Research Studies Press Ltd.
- Mayer, W.J., Lechman, D.C., Hilden, D.L. (1980). The Contribution of Engine Oil to Diesel Particulate Emissions. *SAE Paper 800256*.
- Merkisz, J., Mazurek, S. (2007). *Pokładowe systemy diagnostyczne pojazdów samochodowych*. Warszawa: Wydawnictwa Komunikacji i Łączności.
- Novel-Cattin, F., Rincon, F., Trohel, O. (2000). Evaluation Method for Diesel Particulate Trap Regeneration Additives: Application to Fire Additives. *SAE Paper 2000-01-1914*.
- Pehan, S., Jerman, M. et al. (2009). Biodiesel influence tribology characteristics of a diesel engine. *Fuel*, 88(6), 961-1152.
- Pehan, S., Jerman, M. et al. (2009). Biodiesel influence tribology characteristics of a diesel engine. *Fuel*, 88(6), 970-979.
- Quigley, R., Barbour, R., Fahey, E., Arters, D., Wetzel, W., Ray, J. (2009). A Study of the Internal Diesel Injector Deposit Phenomenon. TAE, Fuels 7th Annual Colloquium.
- Sadle, J. (2002). *Spektroskopia molekularna*. Warszawa: Wydawnictwa Naukowo Techniczne. Stanik, W., Jakobiec, J., Wądrzyk, M. (2015). Wpływ stabilności termooksydacyjnej
- biokomponentów na pracę układu wysokociśnieniowego wtrysku paliwa typu Common Rail. *Logistyka*, *5*, 569-576.
- Stanik, W., Jakóbiec, J., Wądrzyk, M. (2013). Design factors effecting the formation of the air-fuel mixture and the process of combustion in compression ignition engines. *Combustion Engines*, *3*, 40-50.
- Wickström, A. (2012). Variable Valve Actuation Strategies for Exhaust Thermal Management on a HD Diesel Engine. Stockholm, Sweden: Master of Science Thesis.
- Wiedemann, B.W., Neumann, K.H. (1995). Vehicular Experience with Additives for Regeneration of Ceramic Diesel Filters. *SAE Paper 850017*.

LONG-TERM FORECASTING IN TECHNICAL FACILITIES MANAGEMENT SYSTEMS

Jerzy Korostil¹

¹ University of Applied Sciences in Nowy Sącz, Faculty of Engineering Sciences, Zamenhofa 1A, 33-300 Nowy Sącz, Poland; e-mail: jkorostil@ans-ns.edu.pl

Abstract: The paper analyses the parameters that characterize the state of the safety level of a technical object. The technological object, in addition to the technical object itself, includes information management tools and several components aimed at detecting and counteracting external factors that negatively affect the process of system functioning. To identify the factors that are external dangerous events, methods of forecasting such events are used, which are implemented in the relevant components. All possible events are divided into two types. Events, the impact of which, after being detected fusing forecasting, can be eliminated, and events that have a stronger negative impact on the technical object, which leads to a decrease in the object's security level. The method of long-term forecasting is used to identify the second type of events. This forecasting method is implemented in two stages. At the first stage, starting from the final state of the object, which is critical or catastrophic, the transition is carried out in separate steps, starting from the critical state to the initial state of the object's security level. This procedure is implemented based on the use of data obtained at the stages of tests, testing and experimental operation of the object. The second stage consists in the implementation of intermediate forecasting for each subsequent cycle, the continuous functioning of the technological process, which is much longer than the period of short-term forecasting. If the corresponding, predicted event occurs, then its impact on the object leads to a change in the state of the object. A certain number of such changes can lead to the transition of the object to a critical state. The implementation processes of the two stages are displayed by two lines in the phase system, which displays the current states of the object and represents the process of long-term forecasting. The end point of the first stage and the starting point of the second stage coincide. The value of the distance between the current points of the two lines corresponding to the selected time point of the object's operation allows us to estimate the possible value of the change in the level of the dangerous state, which may occur in the next period in relation to the current cycle of the object's operation. The fragment of the line of the second stage, for the cycle of operation, on which the occurrence of the event of the second type is expected to be predicted, is formed on the basis of the selected method of its extrapolation.

Keywords: forecasting, security status, object status parameters, event, security measure.

Introduction

When designing systems of technical objects (STO_i) and corresponding technological processes $(Pr_i(TO_i))$, the tasks of determining the term and conditions of their safe operation arise. The basic parameters used to solve this problem are the resource of the corresponding technical object $Rs_i(TO_i)$, the reliability of operation $Pr_i(TO_i)$ and a number of other more specialized parameters, that reflect those or other features of the functioning of $Pr_i(TO_i)$. Analysis of the possibilities of long-term functioning, for the majority of $Pr_i(TO_i)$, is a rather relevant and difficult problem. Therefore, in many cases, the size of the resource is determined by various physical measures. An example of this can be TO_i of the type of aircraft, for which the resource is determined by the number of hours during which the aircraft performed flights, for

cars, such resource is determined by the number of kilometers that the corresponding vehicle traveled, and others (Młyńczak, 2012). The resource cannot take into account and recognize all possible types of factors affecting the functioning of $Pr_i(TO_i)$. For different TO_i , the corresponding factors may be different. Confirmation of the insufficiently substantiated use of a limited number of general parameters, to assess the possibility of extending the operation time of TO_i , is the performance of work on the extension of the resource, for selected groups of TO_i . In this case, only internal factors arising within the framework of TO_i itself are taken into account. Such an approach may determine the possibility of further operation of TO_i in the conditions in which it was operated before the work on the extension of the resource. This significantly reduces the versatility of renewable TO_i . One of the solutions to this problem is to carry out design work on the modernization of the corresponding TO_i , but this cannot ensure a certain level of safety of the operation of TO_i . When performing work on the extension of the resource, it is necessary to additionally determine the degree of influence of various factors on the value of safety, which significantly complicates the implementation of the corresponding work. In order to streamline the methods of assessing the possibility of ensuring the safe functioning of $Pr_i(TO_i)$, it is necessary to expand the number of general parameters characterizing the state of the technical object system STO_i and to develop a method of long-term forecasting (LFT) of the occurrence of dangerous situations in $Pr_i(TO_i)$.

1. Determination of parameters characterizing the state of the technological process

The parameters that characterize the technological process and directly determine their critical or catastrophic state include:

- a) resource (Rs_i , resource) of the technical object,
- b) diagnosticity (Dg_i , diagnosis), which determines the ability to detect internal malfunctions occurring in TO_i ,
- c) reliability (Rl_i , reliability) functioning of the technological process,
- d) resistance (Re_i , resistance) in relation to external factors that negatively affect $Pr_i(TO_i)$,
- e) safety (Sf_i , safety) operation $Pr_i(TO_i)$),
- f) catastrophe (Ct_i , the catastrophe) of technological proces $Pr_i(TO_i)$.

The above parameters refer to the STO_i system, which consists of hardware tools, algorithmic tools and physical components that provide the possibility of implementing within the framework of $Pr_i(TO_i)$ the necessary processes of a natural nature (physical, chemical, biological and other). Let's consider the definitions that represent the interpretation of the given parameters, within the framework of which they will be used.

Definition 1. The resource parameter Rs_i , in most cases, determines the physical ability of TO_i , to provide the ability to implement the algorithms of the corresponding $Pr_i(TO_i)$, which is measured by a time interval covering the entire process functioning of STO_i .

One of the interpretations of the resource parameter is the time interval of safe operation TO_i , which is calculated when designing TO_i . Such a time interval can be determined by the number of work cycles or the number of hours of work in the prescribed time interval with a nominal load (Lindstedt, Sudakowski, Grądzki, 2016).

The peculiarity of using this parameter is its association with technical and natural components TO_i . Therefore, the resource parameter is dominant, since the change in the value of this parameter can directly affect the change in the general state of the system STO_i . An important feature of the resource parameter is that, in most cases, the resource cannot increase within the framework of the system's functioning processes. Such an increase is possible only in case of preventive or repair work with TO_i . The resource size parameter is a mandatory parameter for all designed TO_i .

Definition 2. The diagnosability parameter Dg_i of the system describes the degree of its ability to detect and counteract the negative impact of random internal factors or malfunctions that may occur in STO_i .

In most cases, separate diagnostic systems are used in STO_i . The value of the parameter Dg_i can be influenced by modifying the informational, technical, or physical components of the system. This influence is aimed at expanding the capabilities of the diagnostics system (SD_i) in detecting and eliminating malfunctions occurring in STO_i (Korbicz, Kościelny, Kowalczyk, Cholewy, 2002).

Definition 3. The reliability parameter Rl_i determines the algorithmic ability of TO_i to implement processes $Pr_i(TO_i)$, which are determined by algorithms that are implemented by information means and selected methods of implementing physical and other natural processes that supposed to be used in STO_i .

In contrast to the resource, the reliability parameter determines the ability to function $Pr_i(TO_i)$ in accordance with the intended method. The value of reliability can change as a result of deviations in the input data used by the algorithms of the $Pr_i(TO_i)$ process, which determines the possibility of changing the logic of the system's functioning. During the operation of $Pr_i(TO_i)$, as a result of the influence on $Pr_i(TO_i)$ of external factors, it may be necessary to change individual fragments of the logic of the operation of processes that could not be foreseen during the design of STO_i . This also leads to a change in the value of Rl_i .

Definition 4. The system resistance parameter Re_i describes the measure of its ability to counteract the negative impact of random external events (Vp_i) on $Pr_i(TO_i)$.

This parameter is based on the use of means of predicting the occurrence of events Vp_i that negatively affect the STO_i system and methods of countering their negative impact (Ławryńczuk, 2022).

Definition 5. The parameter characterizing the security of the system STO_i in relation to known dangers Sf_i that exist in the surrounding environment and can activate corresponding attacks on STO_i , determines the degree of protection $Pr_i(TO_i)$ from these dangers.

The problem of ensuring the safety of the operation of STO_i is solved at the stage of designing all components of the system. Mostly, all types of systems use informational, electronic and other means, with the help of which algorithms for managing the entire object are implemented. In the part of the information component, information protection tools are used, which are widely developed in information systems serving various types of STO_i (Stallings, 2000; Stallings, Brown, 2018). Since processes of different nature can be used in STO_i , during their design, corresponding protection means are simultaneously

created. Methods of implementation of means of protection depend on the type of their physical nature. There can be many natural processes used in STO_i . These can be physical, chemical, biological and other processes.

Definition 6. The parameter characterizing the negative state (NCn_i) of the STO_i system is determined by parameters whose values change over a short time interval and become close to their extreme values.

A catastrophe of the system STO_i will be called such a state of it, in which the values of the parameters of the system state take their extreme values in a short time interval (Janeczko, 2012; Bity, 2016). For technical systems, the occurrence of catastrophic states is a fairly common phenomenon. The concept of a short time interval during which the state of the technical system changes is relative. The value of such a time interval is determined based on a comparison of the speed of such changes with the real-time speeds of the functioning processes of the corresponding $Pr_i(TO_i)$.

2. Analysis of technological process state parameters

The parameters $P_i(STO_i)$ of the general state of the system (GCS_i – the general state of the system), which implements the technological process, differ from the parameters $Pa_i(STO_i)$ of the system functioning processes (PPF_i). The PPF_i parameters have accepted measurement units related to the nature of these processes. The GCS_i parameters of the $Pr_i(TO_i)$ process, in most cases, have only a qualitative interpretation and allow their numerical evaluation by the number of factors characteristic of them. Dependencies between changes in the values of PPF_i and GCS_i cannot always be established unambiguously. The parameters PPF_i directly describe the processes of functioning $Pr_i(TO_i)$ during time t, for example, temperature parameters, speed of revolutions, others, parameters GCS_i describe, in general, the state of STO_i during throughout the system's operation time. To determine the state of the system STO_i , the parameters Rs_i , Rl_i , Dg_i , Re_i and Sf_i are used, the values of which determine the value of the parameter NCn_i , or Ct_i . In general, such a dependence can be written in the form:

$$Ct_i(STO_i) = \mathcal{F}(Rs_i, Rl_i, Dg_i, Re_i, Sf_i, t)$$
(1)

The change in the states of the STO_i system is reflected in the phase space, since it is rather difficult to interpret the values of the variables in formula (1) by known physical measures. Consider the possibility of establishing dependencies between individual state variables STO_i based on their interpretation and the introduced conditions that limit the possibility of ambiguity of the corresponding interpretation.

Condition 1. The parameter Rs_i changes during the functioning of $Pr_i(TO_i)$ and, basically, determines the degree of suitability of the hardware component, the physical elements of the system STO_i , to ensure the necessary functioning process of $Pr_i(TO_i)$.

Condition 2. Parameter Dg_i determines the measure of effectiveness of the diagnostic processes of the STO_i system, which consist in the control of diagnostic and technological parameters of hardware components, physical elements, processes and other components of the STO_i system and the measure of effectiveness of the implementation of impact elimination processes malfunctions in the technological process.

Conditions (1) and (2) allow the parameter Rs_i , Dg_i to be linked together, and allow the possibility of interpretations of interdependencies between these parameters. This interpretation means that the diagnostic system (SD_i) detects an event that occurs as a result of the occurrence of a fault in STO_i . It is assumed that the corresponding malfunctions are related to the hardware components of STO_i . If SD_i cannot counteract the negative impact of the corresponding malfunction on $Pr_i(TO_i)$, then the value of the parameter Dg_i decreases and the value of $\Delta\rho_i$ and, accordingly, the value of the parameter Rs_i also decreases by, which is different from $\Delta\rho_i$. Thanks to conditions 1 and 2, it becomes possible to depend on the partial change of the quantity Rs_i on the change of the quantity Dg_i . Thanks to this, it is possible to reduce the dimensionality of the phase space.

The reliability parameter characterizes the ability to perform the necessary functional process $Pr_i(TO_i)$ described by algorithms (Al_i) in the case when they are affected by negative information factors. This means that the parameter Rl_i can characterize the algorithmic capabilities of STO_i , which are implemented by the system $(\mathcal{L}(STO_i))$ which is a set of individual algorithms Al_i , which can be written in the following form:

$$Pr_i(TO_i) = \mathcal{L}(STO_i) = \mathcal{L}(Al_1, \dots Al_n)$$
 (2)

Let's formulate a hypothesis.

Hypothesis 1. Algorithmic means implemented in $Pr_i(TO_i)$ cannot take into account all cases that may lead to negative factors affecting $\mathcal{L}(STO_i)$ and lead to deviations in the functioning of the process $Pr_i(TO_i)$.

It is known from the theory of protection of information systems that unauthorized modifications of algorithms in information means are implemented using known attacks on information systems. Thanks to this, it is possible to combine the Rl_i parameter with the Sf_i parameter, which protects the information components of the system from external attacks. Therefore, to determine the method of implementing forecasting, it is possible to limit yourself to two parameters Re_i and Sf_i .

Interrelationship of Ep_i with $Pr_i(TO_i)$ is carried out by interaction of parameters of the external environment $(Ep_{ij}(Ep_i))$ with system parameters STO_i . Such parameters may be different for different STO_i . Their interaction with STO_i may depend not only on the type of parameter $Ep_{ir}(Ep_i)$, but also on the value of this parameter.

The system resistance parameter Re_i is focused on determining the necessary degree of protection $Pr_i(TO_i)$ from each random event Vp_i , characterized by the possibility of a negative impact on $Pr_i(TO_i)$.

This parameter is one of the characteristics of the security measure value of the entire process $Pr_i(TO_i)$. The magnitude of the resistance measure depends on the capabilities of the hybrid forecasting system SPG_i , which predicts the occurrence of Vp_i and protects the technological process $Pr_i(TO_i)$ from the negative impact of Vp_i on $Pr_i(TO_i)$ (Korostil, Afanasyjewa, Korostil, 2022; Maciąg, Pietroń, Kulka, 2013). Such means, based on the use of forecasting methods, determine the time of occurrence of Vp_i and their individual parameters, the specifics of their impact on the object of protection and implement the necessary countermeasures to such an impact. All these functions are implemented by the hybrid forecasting system SPG_i , which is characterized by the efficiency parameter π_i .

The parameter characterizing the security value Sf_i differs from Re_i in that the protection means have information about known threats and processes of negative impact on the protection object. Thanks to this, the object protection system (SDO_i) detects and recognizes attacks activated by threats. Based on this data, SDO_i selects among the available defenses those that counter the corresponding attacks.

An important difference between the system for predicting negative events and counteracting them, which is characterized by the parameter Re_i , from the protection system characterized by the parameter Sf_i , is as follows. In the first case, the SPG_i forecasting system performs preventive actions that may prevent negative impact on the object. In the second case, to counteract the negative impact on the process $Pr_i(TO_i)$, it is necessary to recognize it at the initial stages of its implementation and only after that it becomes possible to counteract the development of a negative impact on the object of protection. Based on recognized data, SDO_i assesses the level of danger of negative impact on the object and implements appropriate countermeasures. The parameter Sf_i is used to evaluate these factors.

3. A method of predicting the change in the security state of a technical object

To determine the method of detecting the possibility of occurrence of negative states STO_i , it is necessary to introduce several conditions and provisions.

Condition 3. The factors causing the appearance of a negative state STO_i arise in its external, surrounding environment Ep_i .

Condition 4. The means of protection of STO_i do not have all the necessary information at the appropriate moments to counteract the negative impact on STO_i of possible threats.

Provision 1. The influence of the threat $(Tr_i$ -threat) on the system STO_i is implemented by changing the value of the parameter $Pa_i(STO_i)$ which is determined by the threat Tr_i , which activates an attack that uses the corresponding parameter $Pe_i(Ep_i)$.

Threats that can activate a negative impact on STO_i lead to a change in the value of the corresponding parameters of the object's state, which is realized indirectly through a change in the $Pa_i(STO_i)$ parameter.

Long-term forecasting is a process that makes it possible to determine whether a random event (Vd_i) will occur during the forecasting interval $\Delta TDn \gg \Delta T$, which has a negative effect on STO_i , leading to the emergence of dangerous and catastrophic conditions. An extended interpretation of the LTF process is the prediction of a certain event that may occur after a relatively long time interval. In the proposed interpretation, the LTF process functions during a number of time intervals of system operation starting from the moment of its activation until the moment of completion of the last, regular stage of operation STO_i . This interpretation is due to the fact that it is not advisable, having received certain information about the possibility of occurrence of the event Vd_i , to limit oneself to the implementation of counteraction processes, which may not be sufficiently adequate for the real event Vd_i . This means that it is necessary to implement processes that can provide additional information about the possible event Vd_i and about increasing or decreasing the probability of its occurrence. Reaction processes Vd_i must take into account additional information that can be obtained during LTF operation. Such processes will be called intermediate forecasting processes (IFP_i) .

Let us assume that ΔTDn_i is a relatively long prediction time interval during which events Vd_i may occur. Then you can write: $\Delta TDn_i \gg \Delta T_i$ where ΔT_i is the time interval during which the event Vp_i occurs. To determine the method of implementation of IFP_i , let's accept the hypothesis according to which during the selected time interval ΔTDn_i the event Vd_i will definitely occur. Otherwise, the IFP_i process is not considered. During the LTF_i process, the analysis of changes in the values of parameters $P_{ik}(Cn_{ij})$ characterizing the state of STO_i is implemented. Negative system states $NCn_{ij}(STO_i)$ critical states Ct_i are known. These states are determined during the design of STO_i and their number can be limited.

The approach to the implementation of LTF_i is carried out in two stages. The first stage IFP_i begins with the selected, known state $Cn_i(STO_i)$, from which we move in separate steps to the current state STO_i , or $TCn_i(STO_i)$, which also is known at time t_i . At this stage, which we will call the reverse stage (RV – revers stage), the process of transition from the final state $Ct_i(STO_i)$ to the current state $TCn_i(STO_i)$ of the system STO_i is carried out, which can be written in the form: $Ct_i(STO_i) \to TCn_i(STO_i)$. At each transition step, the current states Cn_i are selected, the numbering of which is determined by the sequence of indices: $[\cdots \rightarrow (i+1) \rightarrow (i) \rightarrow (i-1)\cdots]$ and the possible values of the parameters of the state Cn_{i-1} and states Cn_i . Based on this, the possibility of transition from state Cn_i to state Cn_{i-1} is established. This possibility is determined at the initial stages of the STO_i tests. In the first step of the RV stage, the state Cn_i corresponds to the state $Ct_i(STO_i)$. Among the various possible options for changing the state STO_i , such a possible transition is selected, which is determined by the event Vd_i , leads to a corresponding change in the parameter characterizing the magnitude of the threat. Therefore, the RV stage will reflect the trajectory of the state change of STO_i , in the phase space, which corresponds to the negative influence of Vd_i on STO_i , which may occur in Ep_i .

At the second stage of the process LTF_i , which we will call the direct stage (DR - direct stage), the transition process is carried out in separate steps from the current state $TCn_i(STO_i)$ to the final state $Ct_i(STO_i)$ of the system STO_i , which can be written in the form: $TCn_i(STO_i) \rightarrow Ct_i(STO_i)$. At each step of the transition, current states Cn_i are determined, the numbering of which is determined by the sequence of indices: $[....\rightarrow (i-1)\rightarrow (i)\rightarrow (i+1)\rightarrow \cdots]$. In this case, the initial data is the data from $TCn_i(STO_i)$, which reflects the initial state of the system STO_i .

Based on the analysis of the discrepancy between the trajectories of state changes between the processes implemented at two stages of forecasting of the LTF_i type, intermediate forecasting estimates IFP_i are determined, which confirm the possibility or not of the occurrence of Vd_i at one or another moment in time functioning of the STO_i system.

4. Realizations of stage RV of forecasting process NCn_i

Upon completion of the design of the technical object, the test stage and the experimental operation stage STO_i are implemented, which allows obtaining initial data that can be used to forecast and determine the values of the system state parameters at the initial stage.

The estimation of values of parameters $P_i(Cn_i) \leftrightarrow \{Rs_i, Re_i, Sf_i\}$ is carried out on the basis of the analysis of the processes that cause changes in their values. The degree of impact of these processes on $Cn_i(STO_i)$ is closely related to the reaction of STO_i to the corresponding impact. A change in the state of $Cn_i(STO_i)$ occurs as a result of the action on STO_i of one or a number of parameters $Pe_i(Ep_i)$, which are interpreted as events Vd_i , which can be written in the form: $Pe_i(Ep_i) \rightarrow [(Cn_i) \lor (NCn_i)]$. We will evaluate the state of the system by the degree of danger of the corresponding state STO_i , which we will call internal danger $(\mathcal{I}d_i)$, or $\mathcal{I}d_i(NCn_i)$. This danger is determined by the amount of change in the values of process parameters $Pr_i(TO_i)$, which can lead to changes in the functionality of the system STO_i . The safe operation process $Pr_i(TO_i)$ corresponds to the case when $Cn_i(STO_i)$ is not in the state NCn_i or Ct_i .

Let's consider the method of assessing the magnitude of the danger, which should be based on the use of numerical values of the parameters of the system state. A change in the value of $\mathcal{Id}_i(NCn_i)$ is caused by a change in the value of one, several or all state parameters STO_i at the same time. For the numerical evaluation of the measure of internal danger \mathcal{Id}_i of the negative state NCn_i , it is necessary to create tables of the values of this measure with a description of the interpretation of the consequences of its influence on the state parameters P_i of the system STO_i . Such a table contains the numerical value x_i of the measure of influence of the internal danger \mathcal{Id}_i , which determines the corresponding state of the system. Thanks to this, it is possible to determine the state of the system by the measure of internal danger $\mathcal{Id}_i(x_i)$. This table describes the interpretation of system states. A certain value of the value of the measure of internal danger can lead to a decrease in the functionality of the corresponding system STO_i . Different state parameters $NCn_i(STO_i)$ can lead to different values of x_{iq} changes. To determine the overall value of the system hazard rate $\mathcal{E}_i(NCn_i)$, the current values of the values of various parameters from the ratio $P_i(Cn_i) \leftrightarrow \{Rs_i, Re_i, Sf_i\}$ are added together, which can be written as:

$$\mathcal{E}_i(NCn_i) = Rs_i(x_{iq}) + Re_i(x_{iq}) + Sf_i(x_{ik})$$
(3)

where the value of each parameter represents some dimensionless numerical value. The possibility of using dependence (3) is due to the fact that each parameter $P_i(Cn_i)$ is determined independently of other parameters. The system state change function described by the value $\mathcal{Id}_i(x_i)$ is a flat line, the curvature of which changes depending on the change in the value $\mathcal{Id}_i(x_i)$. A natural equation describing the curvature of a plane curve as a function of arc length is used to describe such a line. Thanks to this, it becomes possible, for the curves obtained at the stages of RV and DR, to combine their initial and final points.

Consider the implementation of the RV process, which starts from the final state $Ct_i(STO_i)$. According to the hypothesis, the system STO_i during a number of time intervals ΔTD_i will go to the state Ct_i , the parameters of which are known. Intermediate states STO_i in the RV process can be states Cn_i , or negative states $NCn_i(STO_i)$, in which the amount of internal danger \mathcal{Id}_i of the system STO_i changes. Such a transition is carried out in separate steps, at each of which the values of one or a number of parameters of the system state change. Let's assume the following condition for using parameters $P_i(Cn_i) \leftrightarrow \{Rs_i, Re_i, Sf_i\}$.

Condition 5. An increase in the value of the Cn_i parameters always leads to an increase in the danger value of the changed state $NCn_i(STO_i)$, which can be described by the following relationship:

$$\left\{ \mathcal{I}d_{(i-1)}\left(NCn_{(i-1)}\right) \to \mathcal{I}d_{(i)}\left(NCn_{(i)}\right) \right\} \to \left\{ \mathcal{E}_i\left(\mathcal{I}d_{(i)}\right) > \mathcal{E}_{i-1}\left(\mathcal{I}d_{(i-1)}\right) \right\} \tag{4}$$

The operation process of the STO_i system consists of a set of separate intervals of operation. To determine the value of the parameter Rs_i , a time interval is taken, during which all intervals of the functioning processes of STO_i are implemented. You can write a ratio that illustrates the change in the magnitude of the threat measure:

$$\lim_{Rs_i \to 0} \mathcal{I}d_{(i)}(NCn_i) = \{\max_{0 \le \mathcal{E}_i} \mathcal{E}_i(NCn_i) = Ct_i(STO_i)\}$$
 (5)

Forecasting LTF_i is characterized by a number of factors. To expand the understanding of LTF_i , it is necessary to increase the number of possible factors related to LTF_i . Events Vd_i forecasted by LTF_i should be different from events Vp_i forecasted by short-term forecasting (STF_i) .

Statement 1. The influence of Vd_i on the system STO_i is much greater than the influence of Vp_i on STO_i .

According to the definition, the event Vp_i occurs during time intervals ΔT_i , which may be m during one cycle of operation STO_i . The event Vd_i can also occur during one system operation cycle k times, but $k \ll m$ and, accordingly, $\Delta T D_i \gg \Delta T_i$. This is due to the fact that Vd_i is determined by the prediction LTF_i , and the event Vp_i is determined by the prediction STF_i . In order to distinguish the event Vd_i from the event Vp_i , they must be different from each other. Such a difference can only be expressed as a measure of influence on STO_i . Since the negative impact of events on STO_i is considered, to determine the magnitude of such an impact, it is possible to use the value of the measure of the dangerous state $\mathcal{Id}_{(i)}$, to which the corresponding event led STO_i . An event that occurs after a time interval ΔTD_i should take longer to form in the environment Ep_i , which from the point of view of physics can lead to an increase, for example, in such a characteristic as the amount of energy, or another characteristic that determines the degree of influence of Vd_i on the corresponding parameter STO_i . It can be assumed that the events Vp_i and Vd_i can affect the same parameters Pa_i , which are mediators of influence on the system state parameters $Pa_i \rightarrow P_i(Cn_i)$, where $Pa_i = \{Re_i, Sf_i\}$. This is based on the fact that the parameters Re_i , Sf_i determine the state of the system Cn_i , the change of which is the final result of the influence of Vp_i and Vd_i on the system STO_i . Let's assume that the process of the influence of an arbitrary event on STO_i represents the transfer of energy from the carrier Vd_i to the corresponding parameter Pa_i of the system STO_i . Then it can be stated that Vd_i , in relation to Vp_i , should transmit, in the process of influencing STO_i , much more energy than the event Vp_i , if its energy is taken as its characteristic, which means its greater influence on STO_i . This proves the statement.

The parameter characterizing the influence of an arbitrary event on STO_i is the time interval of the impact $\Delta \tau_i$, where $\Delta \tau_i(Vd_i) \gg \Delta \tau_i(Vp_i)$. The influence process is implemented in accordance with the nature of the interaction Pe_i with Pa_i , on the basis of which the characteristics of such interaction can be established.

Statement 2. The period of influence of Vd_i on STO_i is significantly greater than the period of influence of Vp_i on STO_i .

The events Vp_i and Vd_i affect STO_i through the action on one of the parameters $Pa_i(STO_i)$. Each of Pa_i characterizes a fragment of the physical process $Pr_i(STO_i)$, or the process as a whole. Let's assume that the physical processes of impact are interpreted as the transfer of energy from the side exerting influence to the side exposed to influence, the values of the corresponding parameters Pa_i change under the influence of this influence. The transmitted energy, under the negative influence of Vd_i or Vp_i , causes a change in the characteristics of the object, which describe STO_i . The influence of Vd_i and Vp_i is negative, so changes in the corresponding characteristics of the system lead to an increase in the value of $\mathcal{I}d_i$. The nature of the physical reaction process of Pa_i to the impact, for Vd_i and Vp_i is the same, because it is determined by the same parameter Pa_i . Therefore, the time required to transfer a larger portion of energy from Vd_i to Pa_i , compared to the portion of energy from Vp_i to Pa_i , must be much longer. This can be written as the ratio: $\Delta\tau_i(Vd_i) \gg \Delta\tau_i(Vp_i)$, which proves the statement.

The selection of intervals for changing system state parameters at the VR_i stage is implemented on the basis of the data obtained at the initial stages of the STO_i verification, which are tests and experimental operation. At these stages, the final value of the value Rs_i is set. We assume that the change in the values of the quantity Rs_i is described by a non-linear function. In most cases, STO_i prototypes are used for the initial stages, which allows testing in critical and emergency operation modes of STO_i . Intervals ΔTD_i are determined by the value of the operation cycle $Pr_i(STO_i)$. For the initial stages of testing and analysis of the STO_i system, its functioning in critical modes caused by the influence of Vd_i , which are modeled for this purpose, is characteristic. The obtained data about STO_i in such modes of its operation are used to implement the RV stage of the general forecasting process LTF_i .

5. Implementations of the DR stage of the forecasting process NCn_i

The DR stage differs from the RV stage in the following factors:

- the *RV* stage is implemented within the framework of the initial stages, during which trials, testing and experimental operation are carried out;
- the DR stage is implemented in the process of functioning of the STO_i system;
- at the stage of RV, the function $\mathcal{I}d_i(x_i)$ is formed, which determines the change in the measure of internal security of the state STO_i and a number of other differences between RV and DR.

The main function of the DR stage is the implementation of a sequence of event forecasting processes Vd_i , which, unlike Vp_i , can lead to a change in the value of the danger state $\mathcal{I}d_i(x_i)$ of the STO_i system. The intermediate programming process is implemented based on the following conditions.

Condition 6. The occurrence of Vd_i is possible in the case of an increase in the intensity of Vp_i .

At the initial stage, the approximation line for IFP_i is formed based on the use of the function of changing the values of the parameter Rs_i obtained at the initial stage.

Condition 7. The occurrence of local curvature on the line of the IFP_i function is caused by a change in the intensity of occurrence of such Vp_i , which the GSP system could not counteract.

In accordance with statements 1 and 2, the main parameters used for recognition by the IFP_i process of events Vd_i are the parameters of the magnitude of the value Vd_i and the time interval of the influence of Vd_i on the system ΔTDn_i . These parameters increase according to conditions 6 and 7.

The extrapolation line of the event occurrence function Vd_i ($El(IFP_i)$)-extrapolation line), during the operation of STO_i , approaches the display of the function of increasing the intensity Vp_i , increasing the value of the impact measure and increasing the impact time interval Vd_i on STO_i .

An important feature of Vd_i is that Vd_i leads to a change in $\mathcal{I}d_i(x_i)$. The corresponding function is used as an extrapolation function, on the basis of which the IFP_i prediction process is implemented. The IFP_i forecasting system, in addition to the above factors, takes into account additional data about changes in the system that affect the reliability of the IFP_i forecast. An example of such data can be empirical data on changes in the amount of influence and changes in the amount of time of such influence Vd_i on STO_i , depending on the current state of STO_i , or the amount $\mathcal{I}d_i(x_i)$, depending on the number of Vp_i that were not generalized by the SZO_i protection system and other factors that can be determined by the specific properties of individual STO_i systems.

It is assumed that Vd_i are rare events and, therefore, systems for counteracting the influence of Vd_i on the process $Pr_i(STO_i)$ are not considered. The interpolation curve $El(IFP_i)$ is described in the form of a natural equation. This makes it possible to match the $El(IFP_i)$ curve with the El(RV) curve, which makes it possible at the DR stage to determine the deviation of the current state STO_i from the safe state of the system, which is reflected by the El(RV) line constructed at the RV stage. Such matching consists in combining the initial and final points and in using a universal time axis in the phase space El(RV) and El(DR) so that the deviation values of the points selected on the El(DR) and El(RV) axes correspond to each other. Such a deviation can be taken as the predicted difference between the current value $\mathcal{I}d_i(x_i)$ on the line El(DR) and the expected value $\mathcal{I}d_i(x_i)$ on the line El(RV).

If necessary, it is possible to move from the natural equation of the reduced lines to the form of their functional dependence on the parameters of the system state. When moving from individual parameters of the system state to the parameters characterizing the physical interpretation of the corresponding states, it is possible to obtain the values of the parameters of the system state, which have the appropriate units of measurement. These parameters can be used to exert influence that can change the state of the system.

Conclusions

The paper analyses the parameters characterizing the state of the technological process. The proposed parameters characterizing the state of the system are defined. In the process of analysing the parameters of the system state, the features of the proposed parameters were established. Thanks to this, it was possible to connect several parameters, which allowed us to reduce the number necessary for analysing the state of the system. Studies of state parameters are limited exclusively to the influence of external negative factors on the state of the object.

A slightly different interpretation of the long-term forecasting process, which consists of two stages, is proposed. The first of them is the stage of implementation of the inverse process, which is implemented from the selected final state of the object to its initial state. This makes it possible to construct a function of object state changes for the case of a safe operation process, when the object state change corresponds to its technical capabilities. The second stage is implemented from the beginning of the functioning process to the final state of the object, from which the continuation of its functioning is dangerous.

The paper distinguishes long-term forecasting from short-term forecasting. In the first case, one cycle of forecasting is carried out during a separate technological cycle of system operation. In the second case, a number of forecasting cycles are used within one technological cycle of system functioning. In the first case, the possibility of occurrence of the event Vd_i , whose impact on the system can lead to a change in its state, is predicted. In the second case, the possibility of occurrence of the event Vp_i is predicted, the impact of which on the system can be eliminated by appropriate means of protection.

The methods of implementation of the first and second stages of the forecasting process are presented and assertions are proved that prove the correctness of the accepted provisions used in the work.

References

Bity, B. (2016). *Elementy teorii katastrof w zadaniach*. Gliwice: Wydawnictwo Politechniki Śląskiej. Janeczko, S. (2012). *Wybrane zagadnienia teorii katastrof*. Warszawa: Oficyna Wydawnicza Politechnika Warszawska.

Korbicz, J., Kościelny, J., Kowalczyk, Z., Cholewy, W. (2002). *Diagnostyka procesów. Modele. Metody sztucznej inteligencji. Zastosowanie*. Warszawa: Wydawnictwo Naukowo-Techniczne.

Korostil, J., Afanasyjewa, O., Korostil, O. (2022). Forecasting in technical facility control system. *Journal of Engineering, Energy and Informatics*, 2, 63-75.

Lindstedt, P., Sudakowski, T., Grądzki, R. (2016). *Eksploatacyjna niezawodność maszyny i jej teoretyczne podstawy*. Warszawa: Wydawnictwo Instytutu Technicznego Wojsk Lotniczych.

Ławryńczuk, M. (2022). Nonlinear predictive control using Wiener models: computationally efficient approaches for polynomial and neural structures. *Studies in Systems, Decision and Control, 389*. Cham: Springer.

Maciąg, A., Pietroń, R., Kulka, S. (2013). *Prognozowanie i symulacja w przedsiębiorstwie*. Warszawa: PWE.

Młyńczak, M. (2012). *Metodyka badań eksploatacyjnych obiektów mechanicznych*. Wrocław: Oficyna Wydawnicza Politechniki Wrocławskiej.

Stallings, W. (2000). *Network security essentials. Applications and standards*. New Jersey: Prentice HALL.

Stallings, W., Brown, L. (2018). Bezpieczeństwo systemów informatycznych (t. I-II). Gliwice: Wydawnictwo Helion.

APPLICATION OF CHROMATOGRAPHIC SEPARATION METHODS IN QUALITATIVE DATA ANALYSIS FOR SELECTED DATA SETS

Mariusz Święcicki¹

Abstract: Nowadays, one of the important problems related to data mining is the processing of large data sets. In this chapter an algorithm is presented that may apply to issues related to the classification of large-volume data sets. The motivation to define this type of algorithm was that currently the methods used to process this type of data are subject to several significant limitations. The first significant limitation in the use of classical classification methods is the need to ensure a constant data size. The second type of constraint is related to the data dimension. The last type of limitation that occurs in the use of classic classification algorithms is related to the situation that a given input vector may contain data belonging to many classes at the same time, in which case we are talking about so-called multi-class vectors.

The chapter shows an attempt to solve the above problems by defining a classification algorithm inspired by the resolution chromatography method The algorithm is inspired by the method of chromatographic separation of substances, which is used in analytical chemistry.

The chapter presents an algorithm for chromatographic data separation, which was inspired by one of the methods of analytical chemistry, which is resolution chromatography.

Keywords: natural computing algorithms, chromatographic separation, signal processing, data mining.

Introduction

The article presents an algorithm that can be used in issues related to the classification of large-scale data sets. The motivation to define this type of algorithm was the fact that currently the methods used to process this type of data are subject to several significant limitations (Reinsel, Gantz, Rydning, 2017).

Multiclass vector

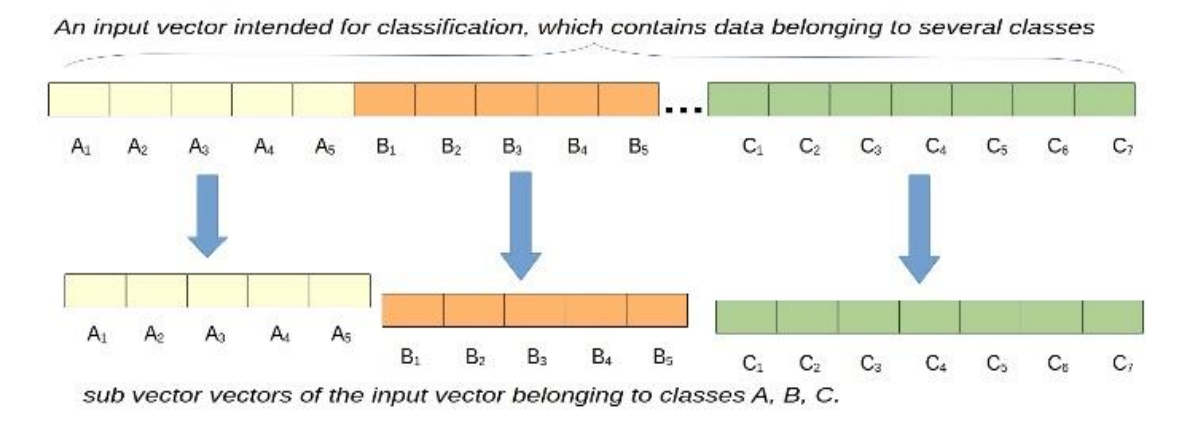


Figure 1. Multiclass vector structure.

¹ Cracow University of Technology, Warszawska 24, 31-155 Cracow, Poland; e-mail: mariusz.swiecicki@pk.edu.pl

The first significant limitation in the use of classical classification methods is the need to ensure a constant size of data – vectors that will be subject to the classification process. The second type of limitation is related to the dimension of the data. When we use classical methods for classifying large vectors, we always have to reduce the dimension of the input vectors using selected mathematical statistics methods (Hilbert, 2016).

Another limitation of currently used algorithms is that the classified data must be homogeneous, i.e. there can only be one type of data. If images are classified, non-image data whose data source is another phenomenon and which is in some way related to the classified images cannot also be classified as input. Finally, the last type of limitation that occurs when using classic classification algorithms is related to the situation that a given input vector may contain data belonging to many classes at the same time, and then in this article we are talking about the so-called multi-class vectors.

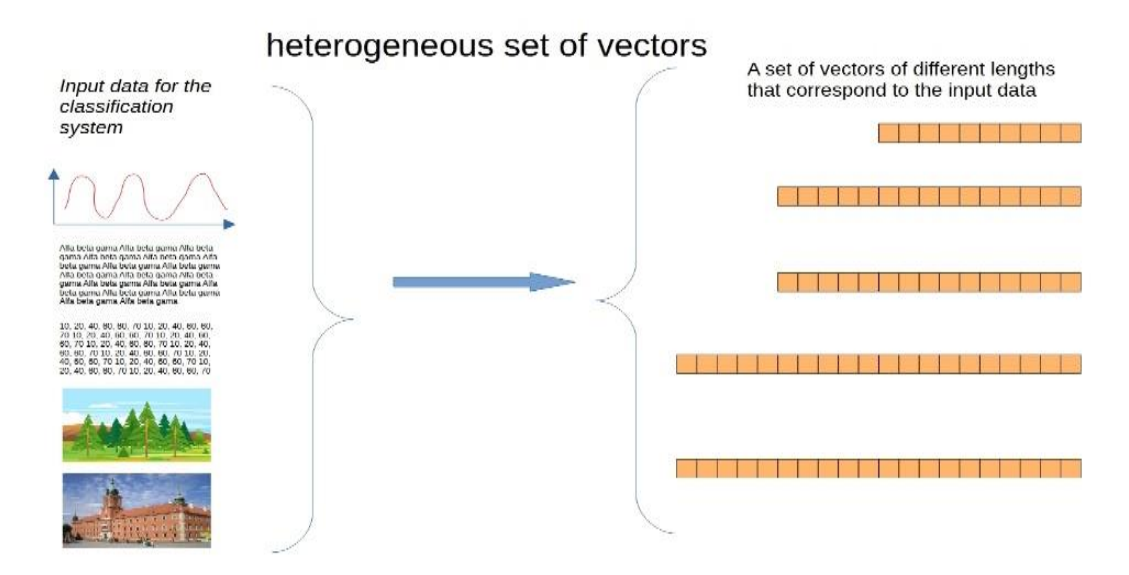


Figure 2. Vector structure of a heterogeneous set of vectors.

The presented algorithm attempts to solve the problems defined above. The presented algorithm attempts to solve the problems defined above. The algorithm is inspired by the method of chromatographic separation of substances, which is used in analytical chemistry. The first chapter of the article will present the principle of chromatographic data separation, which is the basis of the defined algorithm. The second chapter will present an algorithm for data classification, which is inspired by the principles of chromatographic separation of substances. The following parts of the article will present the results of calculations and classification for example data sets.

1. Properties of chromatographic separation of substances

Chromatography – an analytical technique used to separate or examine the composition of mixtures of chemical compounds. In each chromatographic technique, the mixture being tested is first separated and then the individual components are detected. The substance is separated by passing the solution of the tested mixture through a specially prepared separation phase (bed), also called the stationary phase. The separation phase consists of substances that have sorption abilities or can otherwise affect the

flowing substances. The intensity of this process varies for individual components of the mixture. Some components therefore remain in the phase longer and others for a shorter time, which allows them to be separated. The time a given component stays in the column is called the retention time. Generally speaking, chromatographic separation is a process in which a mixture of chemical compounds is separated into at least two fractions with different compositions. From a chemical point of view, the purpose of the substance separation process is to increase the concentration of one of the components of the initial mixture in relation to the remaining components of the initial mixture. Separation takes place using physical methods and chemical reactions (Anon n.d.-a; Bos et al., 2020; Pierce et al., 2021; Varhadi et al., 2020).

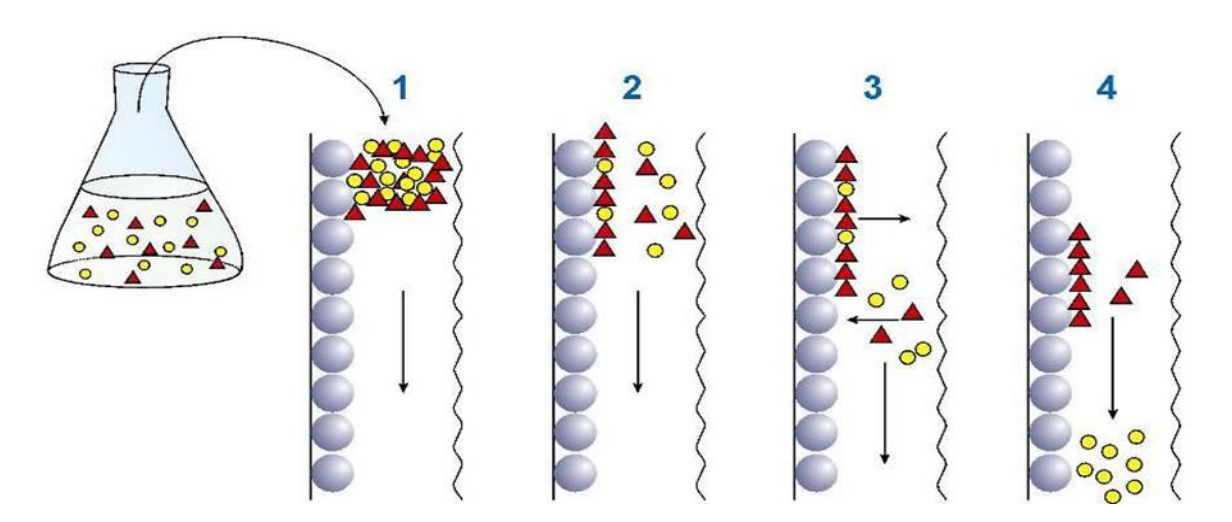


Figure 3. The idea of chromatographic separation of substances.

The Figure 3 presents the chromatograph process, the idea of separating a mixture using chromatography we can see, that the mixed substance is introduced at the entrance of the chromatographic column. The chromatographic column is filled with a substance or substances that have a different degree of affinity for the substances that are being separated – they have been introduced into the chromatographic column.

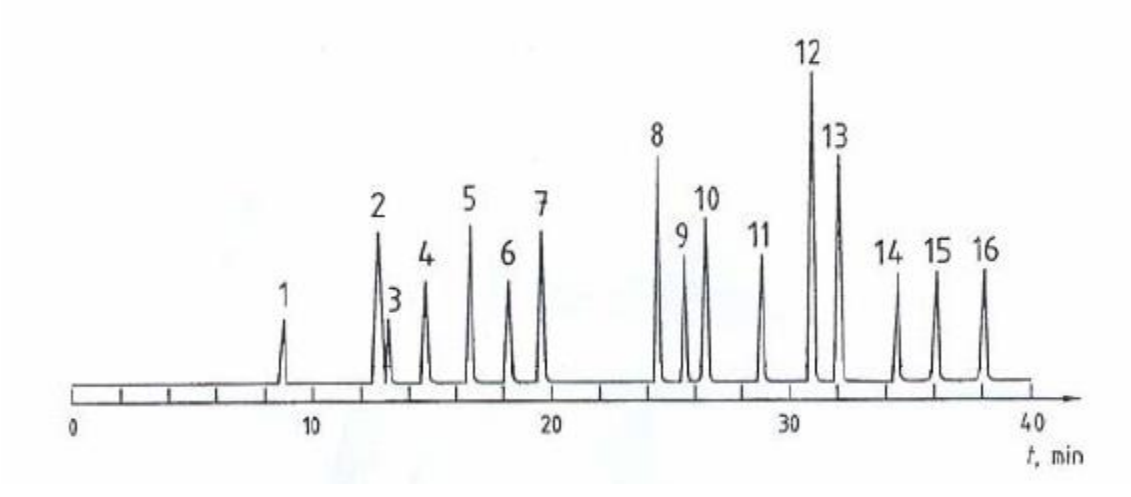


Figure 4. Graph of the substance concentration in the eluate flowing from the column as a function of the elution volume, and when the eluent flow rate is constant as a function of time.

Due to the above, the time it takes for each substance to leave the chromatographic column will be different and will depend on the degree of affinity of a given substance for substances that are in the stationary phase. The output data stream of the chromatograph is the relationship between the concentration of a given substance over time. This relationship is presented by a chromatograph, i.e. a graph showing the relationship between the concentration of a given substance and the time needed to leave the chromatographic column, i.e. the retention time. As is known, the retention time of a given substance is characteristic and depends on the structure of the stationary phase and the structure of the substance being separated.

The chromatographic column is filled with a substance or substances that have a different degree of affinity for the substances that are being separated – they have been introduced into the chromatographic column. Due to the above, the time it takes for each substance to leave the chromatographic column will be different and will depend on the degree of affinity of a given substance for substances that are in the stationary phase. The output data stream of the chromatograph is the relationship between the concentration of a given substance over time. This relationship is presented by a chromatograph, i.e. a graph showing the relationship between the concentration of a given substance and the time needed to leave the chromatographic column, i.e. the retention time. As is known, the retention time of a given substance is characteristic and depends on the structure of the stationary phase and the structure of the substance being separated.

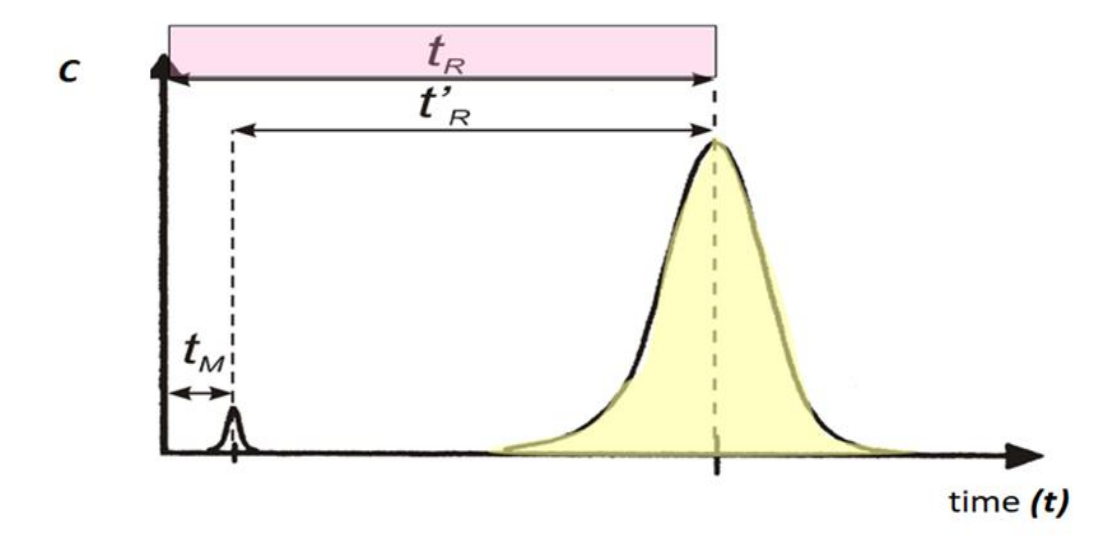


Figure 5. Substance identification: peak position, Peak height: quantification.

Figure 5 shows a signal output generated by the chromatograph. This signal provides two important pieces of information: firstly, it provides information about the type of substance, which is responsible for the retention time – individual for each substance. The second type of information is quantitative information, how much of a specific substance was in the tested mixture. This is determined by the height of the peak, which informs about the concentration of the tested substance at the output of the chromatographic column (Robards, Ryan 2021; Schmidt-Traub, Schulte, Seidel-Morgenstern, 2020).

2. Definition of chromatographic data separation algorithm

The chromatographic data separation algorithm is based on the basic paradigm that the processed data string is a complex chemical molecule with a chain-linear structure. This means that each data vector or set of vectors will be processed by the chromatographic algorithm by the rules that apply in the real chromatographic system.

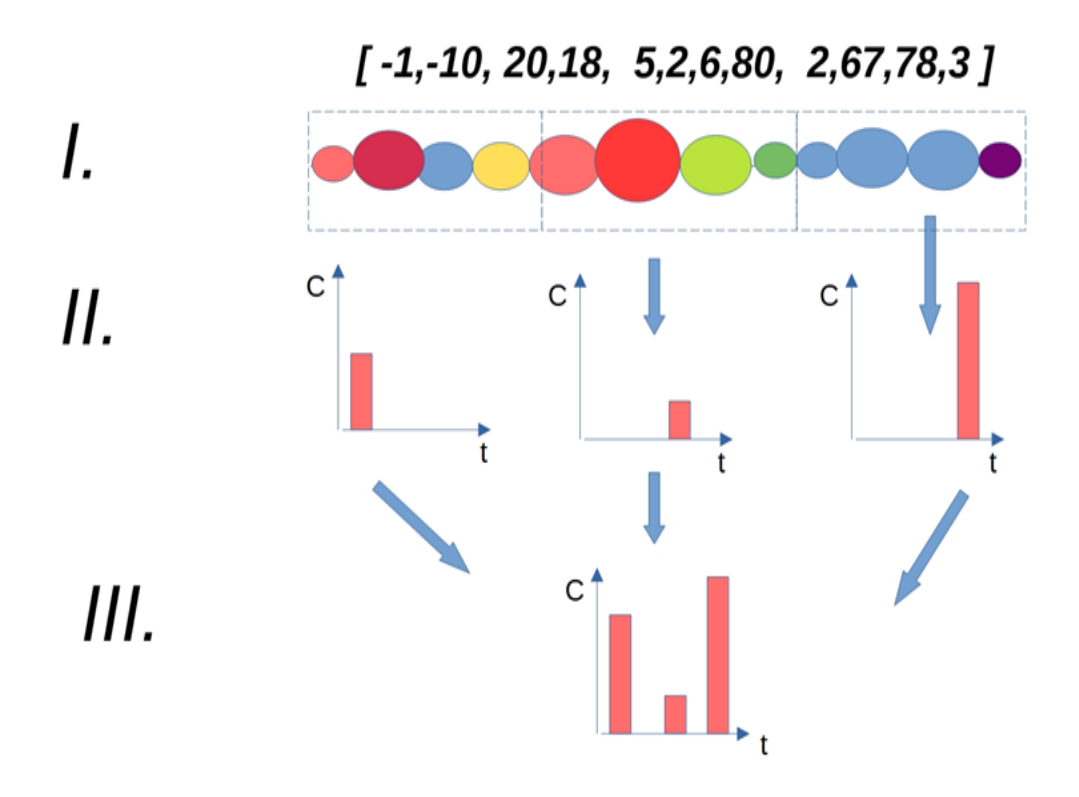


Figure 6. Operations of the chromatographic data classification algorithm.

The general principle of operation of the chromatographic data separation algorithm will be to treat the data vector as a mixture of chemical compounds and for each "chemical" compound the relationship between the concentration of a given substance at the output of the chromatographic system is calculated. In other words, it will involve calculating the spectrum as shown in Figure 6. In the first phase, we treat the vector of numbers as a polyatomic molecule with a linear structure. In the next phase, the molecule is divided into smaller molecules. In the last phase of the algorithm, each newly created molecule is processed by the chromatographic column, i.e. the retention time is calculated. As a result of these operations, a chromatogram is created, i.e. a graph describing the concentration of a given type of molecules as a function of time at the output of the "chromatographic" column. This relationship, i.e. the chromatogram, is later called the spectrum of a given starting substance.

The chromatographic data separation algorithm consists of the following sequence of operations, which are inspired by the functioning of a real chromatographic system:

- 1) Mixture creation phase for a given vector
- 2) Retention time calculation phase
- 3) Chromatogram creation phase
- 4) Phase of the analysis chromatogram.

2.1. The phase of creating a mixture for a given

In the first phase of this algorithm, a set of vectors W consisting of any number of vectors of any length is transformed into a set of mixtures of substances through the process of dividing the fragmentation into smaller vectors of the same length. The fragmentation of the vector takes place in such a way that for each element from the set W, a mixture of substances is created that corresponds to this element of the set W.

Input data

 $W=\{w_1,w_2,w_3...w_N\}$ – a set of data vectors that will be processed

Output data

set of substances MS_i , that have been processed by a chromatographic column, i.e. they have a calculated retention time t_r

 $MS_{i..M}=[];$

 $W=\{w_1, w_2,w_M\}$

Foreach w e W

 $1 \quad \text{For a given } w_i \text{ data vector, create a mixture of substances - it will fragment the vector into sub-vectors of constant length} \\$

 $MS_i = \{s_1, s_2,s_{M(i)}\}\$

 MS_i -a set of substances is created by dividing a vector into sub-vectors according to the adopted principle of division,

 ms_i - the elements of this set is the set of substances resulting from the division of the vector w_i , this means that the set will contain individual substances s that are not subject to further subdivision $ms_{M(i)}$:= $\{s_1, s_2,s_{M(i)}\}$ a substance that was created by splitting the wi vector. w_i

- 2 Foreach s e msi
- 3 Calculate Retention Time i t_r the residence time of the substance in the stationary phase
- 4 End End

Algorithm 1. Algorithm transforming a set of vectors into a set of chromatograms.

As shown in the algorithm presented above, the set of mixtures of substances that has been created is fed to the input of a "virtual chromatographic column" in which the process of migration of a given substance between the stationary phase and the mobile phase takes place.

2.2. Phase of calculating the retention time

The value of the retention time t_r depends on the affinity of the stationary phase for a given substance, which is an important value in the classification process. It is known that the value of the retention time depends on the affinity of the substance for the stationary phase that is filled in the chromatographic column. The final fragment of Algorithm 1 contains a sequence calculating the retention time value.

2.3. Chromatogram creation phase

The next stage of the presented algorithm is to create a chromatogram for a given mixture of substances that corresponds to the w_i element. The chromatogram is created as a result of the registration of individual substances at the output of the chromatographic column. The moment at which a given substance will leave the chromatographic column depends on the retention time t_r . The purpose of the detector is to count the molecules of substances leaving the chromatographic column at a given moment of time.

Input data

For a given set of substances MS_i , that have been processed by a chromatographic column, i.e. they have a calculated retention time t_r

Output data

 $CH = \{ch_1, ch_2, ch_3....ch_N\} - a$ set of chromatograms, where each element of this set represents a chromatographic spectrum corresponding to a given element of the set W $ch_i = \{peak_1, peak_2, peak_3....peak_M\} - Each chromatogram consists of a set of peaks$

 $ch_i=[];$

For each s & MSi

peaki[s.Tr]:=peaki[s.Tr]+1

End

Algorithm 2. Algorithm for creating a ch_i chromatogram for a mixture belonging to the w_i vector.

To sum up, the operation of the two algorithms presented above, which model the processes occurring in a real chromatograph, can be presented below in a formalized notation that will later be used in the analysis of the algorithm. Let us assume that the stationary phase FS is an m-element vector as shown in equation (1), while the substance vector that was created as a result of the algorithm in the fragmentation process as a result of the operation of the first algorithm 1 is also an array with dimensions NxM presented in equation (2).

$$FS = (fs_1, fs_2, fs_3 \dots fs_M)$$

$$S = \begin{bmatrix} s_{1,1}, s_{1,2}, s_{1,3} \dots s_{1,M} \\ s_{2,1}, s_{2,2}, s_{3,1} \dots s_{3,M} \\ \dots & \dots \\ s_{N,1}, s_{N,2}, s_{N,1} \dots s_{N,M} \end{bmatrix}$$
(1)

As we know, a chromatogram is made up of peaks, and a single peak is a pair of numbers, the first of which is the retention time tr and the second is the concentration of substance C, formula (3), as the result of the operation of Algorithm 2.

$$peak_i = (tr_i, C) \tag{3}$$

The retention time can be calculated using the F_{tr} function, which calculates the retention time value for a given substance and the vector describing the stationary phase (4).

$$tr_i = F_{tr}(S_{i,1\dots M}, FS) \tag{4}$$

When calculating the retention time, the function calculates the retention time for a given substance taking into account the structure, i.e. the values of the stationary phase. For the purposes of further considerations, it can be assumed that the function calculating the retention time is expressed by formula (5).

$$tr_i = F_{tr}(S_{i,1...M}, FS) = \sum_{k=1}^{M} (s_{i,k} \cdot fs_k)$$

$$\tag{5}$$

As the presented formula shows, the scalar product of two vectors is calculated. The more similar the vectors are to each other, the greater the value of the calculated product, the greater the retention time for a given substance.

2.4. Chromatogram formation phase

The next stage of the presented algorithm is to create a chromatogram for a given mixture of substances that corresponds to the w_i element. The chromatogram is created as a result of the registration of individual substances at the output of the chromatographic column. The moment at which a given substance will leave the chromatographic column depends on the retention time t_r . The purpose of the detector is to count the molecules of substances leaving the chromatographic column at a given moment of time.

The process of detecting a substance that leaves the chromatographic column is presented in the algorithm above. The result of this algorithm is the creation of a ch_i chromatogram for the element w_i .

2.5. Spectrum analysis phase

The last stage of recognizing substances that have been processed by the chromatographic system is the stage of classifying the output chromatographic spectrum and assigning it to the spectra of known substances.

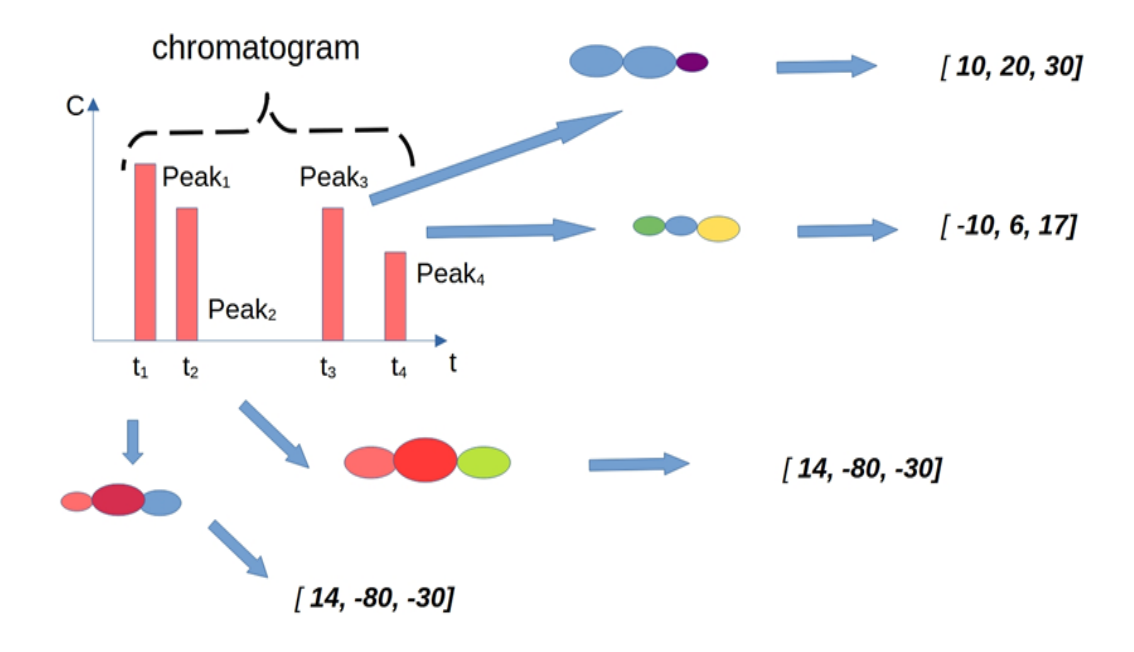


Figure 7. Structure of the chromatogram – the spectrum corresponding to the w_i vector.

The chromatogram of the tested mixture of substances describes the concentration of individual compounds that constitute the composition of the tested substance and which were separated as a result of the chromatography process, similarly to the presented algorithm. As shown in the figure above, as a result of the chromatography process, we obtain a chromatogram that contains many peaks corresponding to the concentration of "substances" that were created as a result of the operation of algorithm 1. The task of the classification algorithm will be to assign the chx chromatogram to the chromatograms of known vectors, using the matching criterion, which is the retention time peak (Pierce et al., 2021).

```
Input data
    ch_a = \{peak_1, peak_2, peak_3 \dots peak_N\} - a \text{ chromatogram consisting of } N \text{ peaks}
    CH=\{ch_1,ch_2,ch_3....ch_l\}
    ch_i = \{peak_1, peak_2, peak_3....peak_M\} - a \ chromatogram \ consisting \ of \ M \ peaks
    D – Distance a value that determines the level of similarity between the ch_a, and ch_b chromatograms
    NoClass - class number
    NoClass:=0; MinDist:=\infty
2
   Foreach chi e CH
    Foreach peakije ch i
3
   P:=\{peak_i^i|abs(t_r^i-t^x) < eps\}
4
5
    f_i := f_i + sum(peak_i^i)
    f_x := f_x + sum(P)
6
     end
   f_i := f_i / sum(peak_i^i)
8
    f_x := f_b / sum(peak_i^x)
10 d_i:=sqrt((1-f_i)^2 + (1-f_x)^2)
11 D:=D \square d_i
12 end
13 NoClass:=\{i \mid min(D_{1..N}) = D_i\}
```

Algorithm 3. An algorithm for classifying a vector w_x using its ch_x chromatogram.

The input data for this algorithm is the ch_x chromatogram, which will be compared with the elements of the set of CH chromatograms corresponding to individual classes. As follows from the presented algorithm, for each chi element belonging to the set of CH chromatograms, a match to the ch_x chromatogram is calculated. Matching the ch_x chromatogram to the chi chromatogram consists in matching all peaks belonging to the ch_x chromatogram for which the difference between the retention time of the jth peak of the chi chromatogram is smaller than the set value, $i.e.\ eps$. Two values are calculated for those peaks that meet the above criterion.

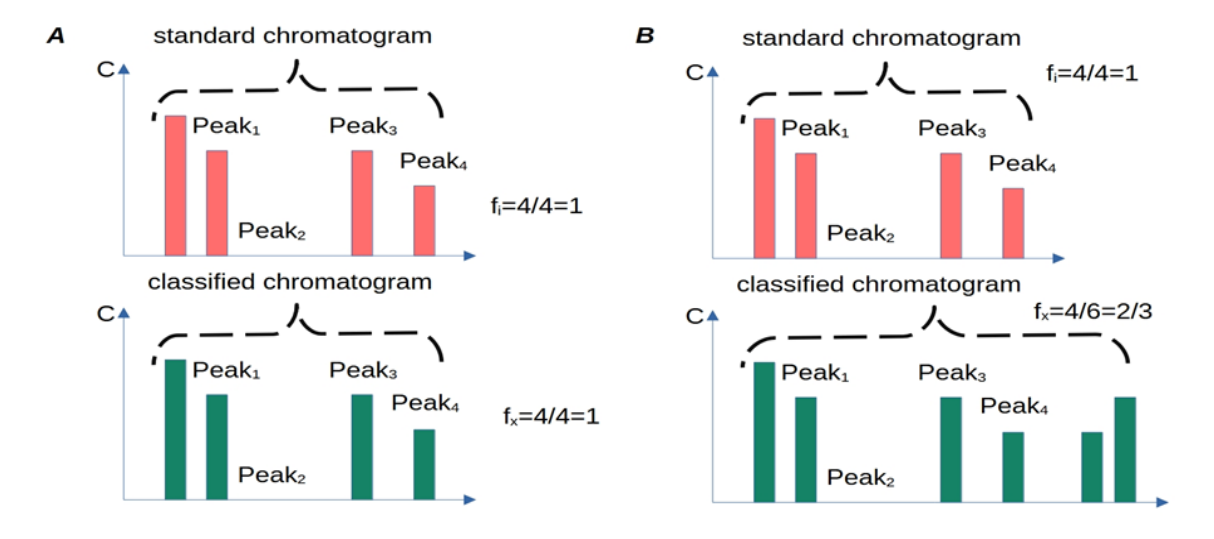


Figure 8. Peak matching process.

Value the phi value (line 8), which specifies the fraction of fitted peaks from the chi chromatogram to the ch_x chromatogram. However, in line 9, the second f_x is also calculated, which contains information about what part of the peaks from the classified ch_x chromatogram was assigned to the peaks from the i-th chromatogram. Line 10 calculates the matching value between the number of matched peaks for the tested chromatogram and the number of peaks matched in the reference chromatogram. As follows from the presented algorithm, the selected chromatogram for which the formula specified on line 10 takes the minimum value means that it will be the chromatogram for which the largest number of peaks belonging to the tested chromatogram were matched and, at the same time, the largest number of peaks were matched in the reference chromatogram.

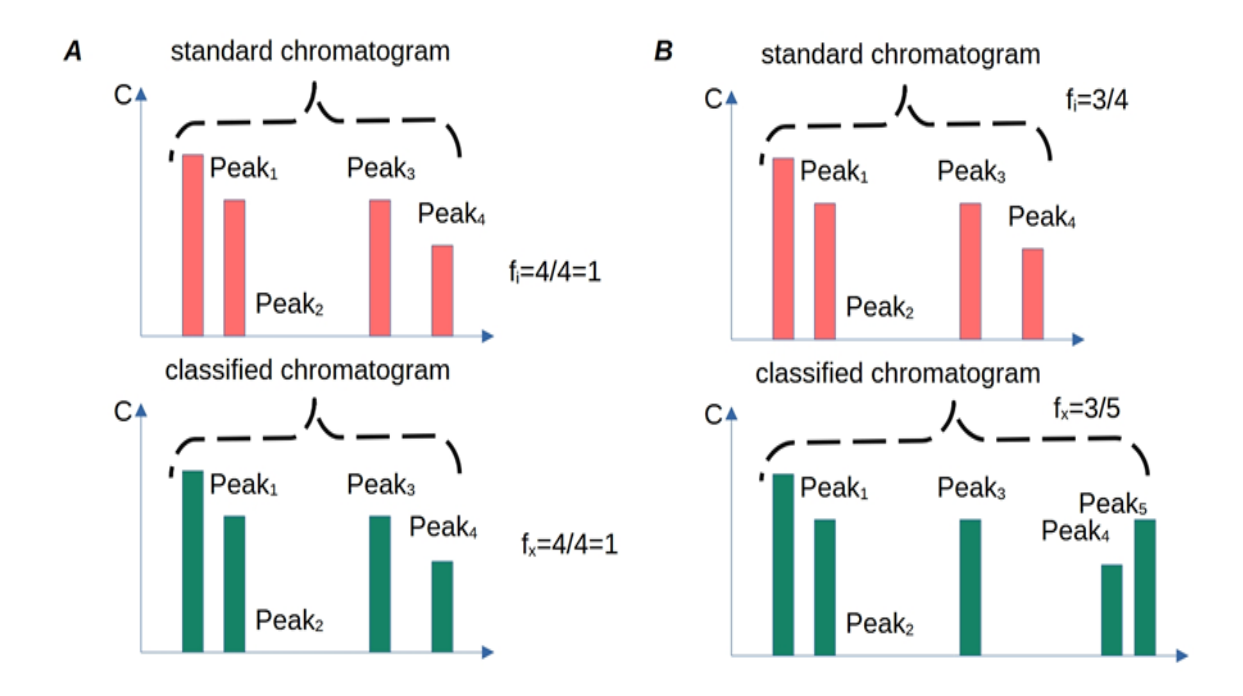


Figure 9. Peak marching process.

The calculation of the f_x and f_i values is shown in the figure above. The Figure 8 shows that if all peaks from the standard chromatogram and the classified chromatogram are matched, then the f_x and f_i values are equal to one, which is shown in the figure in part A. However, part B shows the situation when the classified chromatogram contains more peaks than the reference chromatogram. Then the f_x and f_i values determine the fraction of peaks fitted in the classified chromatogram, and the f_i value determines the number of peaks that were used from the reference chromatogram. The situation as shown in the figure will occur during the classification of multi-class vectors.

The next Figure 9, part B, illustrates the peak matching process when the matching of the classified chromatogram to the reference chromatogram is not complete. This situation occurs when the chromatogram is classified as a result of processing an input vector whose elements have been distorted compared to the standard vector. The algorithm assigns to the classified chromatogram the chromatogram for which the values in line 8 and line 9 reach the maximum value (Anon n.d.-b).

2.6. Problems of selecting the stationary phase

There are two significant problems when performing calculations using the algorithm presented above. The first problem, which was already indicated in the previous chapter, is related to the selection of the stationary phase in such a way that the chromatograms of vectors belonging to different classes are characterized by different retention times. The second problem, in a sense, is a derivative of the first problem, and is related to the fact that the chromatograms that are created in the process are complex, i.e. they contain a large number of peaks, which makes the classification process difficult by the presented algorithm classifying chromatograms.

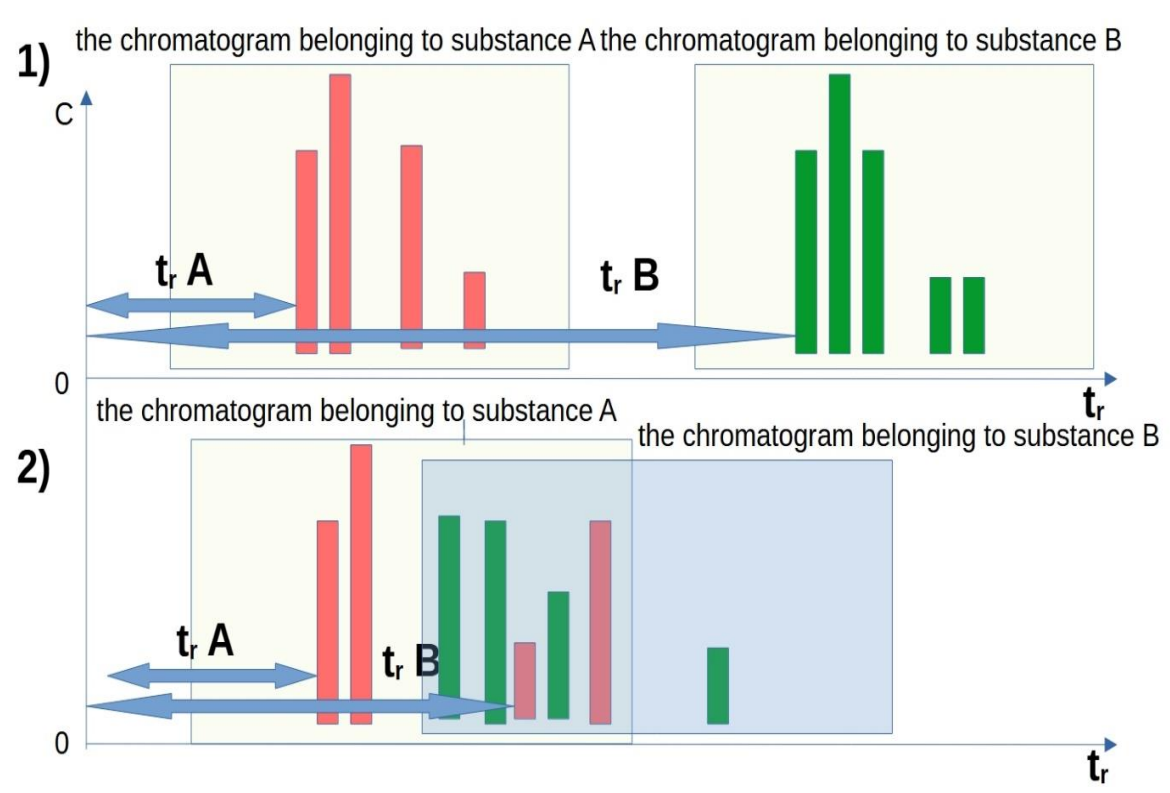


Figure 10. The phenomenon of overlapping retention times.

At this point, an analysis of the functioning of the algorithm will be carried out, taking into account the problem of selecting the stationary phase for a given set of input data vectors, for this purpose the following notations will be introduced.

As the presented formula shows, the scalar product of two vectors is calculated. The more similar the vectors are to each other, the greater the value of the calculated product, and the greater the retention time for a given substance. The description of the algorithm and the drawing above show that the correctness of classification is significantly influenced by the distribution of peaks in the chromatogram of the reference substance as well as in the chromatogram of the classified substance. The optimal situation occurs when the distances between individual chromatograms are large or, in other words, the peaks of individual substances do not overlap. The formula describing the distance between the peaks of the chromatogram is presented in formula (6). This formula describes the distance between the i-th and j-th peak.

$$d_{i,j} = \left(tr_i - tr_j\right)^2 \tag{6}$$

Based on the above-mentioned considerations, a criterion for selecting the stationary layer for a given data set can be defined. The structure of the stationary phase – elements of the FS vector should be selected so that for a given data vector the sum of the distances between peaks is the largest, this relationship is expressed by the formula (7).

$$E(fs_{1}, fs_{2}, fs_{3} \dots fs_{M}) = \sum_{i=1}^{N} \sum_{j=i+1}^{N} d_{i,j}$$

$$\sum_{i=1}^{N} \sum_{j=i+1}^{N} (tr_{i} - tr_{j})^{2}$$
(7)

In other words, the elements of the stationary phase should be selected so that the expression described in formula (7) representing the sum of the distances between peaks has the largest value.

$$max(E(fs_1, fs_2, fs_3 \dots fs_M))$$
(8)

To find the maximum of the function, the conditions presented in formulas (9), (10) must be met.

$$\frac{\partial E(fs_1, fs_2, fs_3, \dots fs_M)}{\partial fs_1} = 0$$

$$\frac{\partial E(fs_1, fs_2, fs_3, \dots fs_M)}{\partial fs_2} = 0$$

$$\frac{\partial E(fs_1, fs_2, fs_3, \dots fs_M)}{\partial fs_M} = 0$$
(9)

$$\frac{\partial^{2} E(fs_{1}, fs_{2}, fs_{3} \dots fs_{M})}{\partial f s_{1}^{2}} < 0$$

$$\frac{\partial^{2} E(fs_{1}, fs_{2}, fs_{3} \dots fs_{M})}{\partial f s_{2}^{2}} < 0$$

$$\frac{\partial^{2} E(fs_{1}, fs_{2}, fs_{3} \dots fs_{M})}{\partial f s_{M}^{2}} < 0$$

$$\frac{\partial^{2} E(fs_{1}, fs_{2}, fs_{3} \dots fs_{M})}{\partial f s_{M}^{2}} < 0$$
(10)

To simplify further considerations and without losing the generality of the conclusions drawn, suppose the stationary phase consists of two elements M=2 and the number of substances for which we want to calculate the chromatogram is four N=4, then the expressions presented above will take the following form:

$$FS = (fs_1, fs_2) \tag{11}$$

$$S = \begin{bmatrix} s_{1,1}, s_{1,2}, \\ s_{2,1}, s_{2,2} \\ s_{3,1}, s_{3,2} \\ s_{4,1}, s_{4,2} \end{bmatrix}$$
(12)

$$E(fs_{1}, fs_{2}) = \sum_{i=1}^{4} \sum_{j=i+1}^{4} d_{i,j}$$

$$d_{1,2} + d_{1,3} + d_{1,4} + d_{2,3} + d_{2,4} + d_{3,4}$$

$$\sum_{i=1}^{4} \sum_{j=i+1}^{4} \{F_{tr}(s_{i,1..M}, FS) - F_{tr}(s_{j,1..M}, FS)\}^{2}$$
(13)

The function that we maximize for a given input set does not have a maximum. A graph of this function for an example data set is shown below.

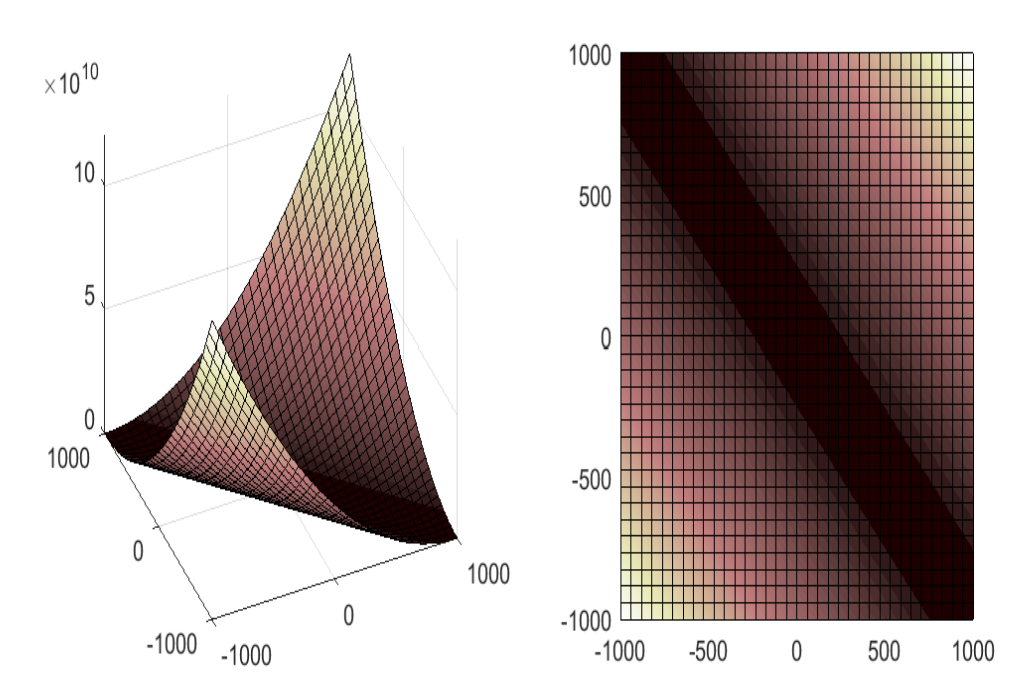


Figure 11. Graph of the maximized function from formula (13) depending on the values of the elements of the stationary phase.

The presented graph shows that the function defined by formula (13) or (7) does not have a maximum in the function responsible for determining the retention time (4), but if the elements of the stationary phase vector have the same sign, the value of function (13) is not limited. This means that the distances between individual peaks will increase proportionally as long as the values of the stationary phase elements increase and if all the stationary phase elements have the same sign. The existence of such a relationship is beneficial, but if we classify highly distorted vectors, the distances between the peaks of the classified chromatogram may differ significantly from the peaks of the chromatogram of the reference vector, which will result in incorrect classification. In this case, replace functions (5) with a non-linear function.

3. Classification of selected data sets

This chapter will present the classification results for two types of data sets, namely for single-class sets and the second type of classification whose results will be presented is the classification of a multi-class set. Both in the case of the first and the second type of classification, the classification will be performed on files that are in a generally available repository and that were used in the process of testing other classification algorithms. It seems that the above conditions are met by the data sets made available on the UCI Repository website. The following collections have been selected. These collections are:

- 1. Letter date set
- 2. Thyroid dataset
- 3. Landsat satellite.

3.1. Classification of a homogeneous and one-class data set

As can be seen from the presented calculation results, the algorithm presented on sample single-class data sets does not differ significantly from other algorithms. The results achieved are average, but it should be emphasized that these are single-class sets with a very small number of attributes. The classified vectors have 16, 32 and 27 attributes respectively.

Table 1
The results of the classification by the chromatographic algorithm

Thyroid Disease Data Set		Landsat Satellite Data set		Letter Recognition		
					Data Set	
Algorithm	%Test	Algorithm	%Test	Algorithm	%Test	
CART tree	99.36	MLP, 36 nodes, +SVNT	91.3	ALLOC80	96.60	
SSV tree	99.33	MLP, 36 nodes,	91.0	K-NN	94.20	
MLP+SCG, 4 neurons	99.24	kNN, k=3, Manhattan	90.9	CHROM dim=1	92.60	
SVM Minkovsky kernel	99.18	CHROM dim=1	90.7	K-NN	92.20	
MLP+SCG, 4 neurons, 45 SV	98.92	FSMneurofuzzy,learn0.95	89.7	LVQ	92.10	
FSM 10 rules	98.90	kNN, k=1, Euclidean	89.4	Quadisc	88.70	
MLP+SCG, 12 neurons	98.83	SVM Gaussian kernel	88.4	CN2	88.50	
Cascade correlation	98.5	RBF, Statlog result	87.9	Bayesian Tree	87.60	
MLP+backprop	98.5	BM $L=31$, $U_a/U_d=10$	87.8	NewId	87.20	
SVM Gaussian kernel	98.4	MLP, Statlog result	86.1	IndCART	87.00	
k-NN, k=1, 8 features	97.3	Bayesian Tree	85.3	C4.5	86.80	
CHROM dim=1	96.1	C4.5 tree	85.0	BM $L=8$, $U_a/U_d=10$	86.56	
Naive Bayes	96.1	SSV tree	84.3	DIPOL92	82.40	
SVM Gauss, C=1 s=0.1	94.7	Cascade	83.7	RBF	76.60	
BP+conj. gradient	93.8	LDA Discrim	82.9	Logdisc	76.60	
1-NN Manhattan,	93.8	Kohonen	82.1	Kohonen	74.80	
SVM lin, C=1	93.3	Bayes	71.3	Backprop	67.30	

The sets from the point of view of the presented algorithm are not well selected – because they have relatively few attributes, but there is a large set of publications presenting the results of the classification of these sets using various classification algorithms.

3.2. Classification of multi class vectors

Using the letter data set, a multi-class set was created – one contains fragments belonging to six classes. The task of the algorithm was to answer the question into what classes a given input vector could be classified.

Table 2
Classification results using a multi-class set chromatographic algorithm

Fragmentation	Number of Classes							
	1	2	3	4	5	6		
16 1D	0.924402	0.733217	0.479568	0.267367	0.115003	0.015178		
8 1D	0.904402	0.703217	0.459568	0.257367	0.100003	0.015178		
4 1D	0.894402	0.693217	0.449568	0.247367	0.09896	0.01478		
16 2D	0.994402	0.803217	0.569568	0.3467367	0.25003	0.0578		
8 2D	0.96789	0.78980	0.506780	0.3098765	0.22003	0.0423		

As the results presented in the table show, the presented algorithm correctly identified three classes – the percentage of correct answers was over fifty percent. However, when indicating the remaining classes to which fragments of the input vector belong, the number of correct answers was not satisfactory.

Conclusions

The article presents an innovative method of data processing similar to chromatographic data separation in analytical chemistry. Three algorithms have been proposed, which aim to convert a data vector into a set of mixtures and classifications of individual chemical substances that were created in the transformation process of the input vector. The paper presents the results of data classification. As has been demonstrated, this data classification technique will be suitable for:

- 1) structured data sets;
- 2) multi-class sets, i.e. those containing fragments, where vectors contain fragments of data belonging to several classes at the same time.

The article presents an algorithm for chromatographic data separation, which was inspired by one of the methods of analytical chemistry, which is resolution chromatography. Three algorithms used in chromatographic data separation have been proposed, which constitute the process of chromatographic data separation. Algorithm 1, is responsible for transforming a set of input vectors into a set of mixtures of substances. Algorithm 2, is the algorithm that is responsible for calculating the retention time. The third algorithm is responsible for assigning the spectrum of the unknown substance, i.e. the input vector, to the chromatograms of the reference vectors. As shown in all the above-mentioned types of datasets, the proposed classification mechanism performed relatively well. To improve the classification efficiency of the presented mechanism, it would be necessary to first algorithmize the problem of selecting the stationary phase taking into account nonlinear functions.

Based on the presented results, it can be assumed that the technique of chromatographic data separation can be successfully used in the processing of large data sets, where the data do not always have such features as a constant length of vectors, a relatively small number of elements in vectors, etc.

References

Anon. n.d.-b. (2024). 'Learning by Simulations: Overlapping Peaks'. Retrieved from: https://www.vias.org/simulations/simusoft_peakoverlap.html.

Hilbert, M. (2016). 'Big Data for Development: A Review of Promises and Challenges'. *Development Policy Review*, 34(1), 135-174. DOI: https://doi.org/10.1111/DPR.12142.

Pierce, K.M., Trinklein, T.J., Nadeau, J.S., Synovec, R.E. (2021). 'Data Analysis Methods for Gas Chromatography'. In: *Gas Chromatography* (pp. 525-546). DOI: https://doi.org/10.1016/B978-0-12-820675-1.00007-1.

Reinsel, D., Gantz, J., Rydning, J. (2017). 'Data Age 2025: The Evolution of Data to Life-Critical Don't Focus on Big Data; Focus on the Data That's Big Sponsored by Seagate The Evolution of Data to Life-Critical Don't Focus on Big Data; Focus on the Data That's Big'.

- Robards, K., Ryan, D. (2021). 'Principles and Practice of Modern Chromatographic Methods'. In: *Principles and Practice of Modern Chromatographic Methods* (pp. 1-518). DOI: https://doi.org/10.1016/B978-0-12-822096-2.09993-X.
- Schmidt-Traub, H., Schulte, M., Seidel-Morgenstern, A. (2020). *'Preparative Chromatography: Third Edition'*. DOI: https://doi.org/10.1002/9783527816347.
- Tijmen, B.S., Knol, W.C., Molenaar, S.R.A., Niezen, L.E., Schoenmakers, P.J., Somsen, G.W., Pirok, B.W.J. (2020). 'Recent Applications of Chemometrics in One- and Two-Dimensional Chromatography'. *Journal of Separation Science*, *43*(9-10), 1678-1727. DOI: https://doi.org/10.1002/JSSC.202000011.
- Varhadi, S.D., Gaikwad, V. A., Sali, R.R., Chambalwar, K., Kandekar, V. 2020. 'A Short Review on: Definition, Principle and Applications of High Performance Liquid Chromatography. *INTRODUCTION*', 19(2), 628-634.

AUTOMATION AND INTEGRATION OF PRODUCTION SYSTEMS IN A MIXED MANUFACTURING ENVIRONMENT – USING FAKRO AS AN EXAMPLE

Wojciech Klimek¹

¹ FAKRO Management Board Member for Production, Węgierska 144A, 33-300 Nowy Sącz, Poland

Although the fourth revolution comes with "industrial" in its name, it has a huge impact not only on what happens in factories, but also on our personal lives. It is reflected in what the industry produces for us, what technologies we use in our everyday lives, what we order, and what expectations we have as customers. Probably not everyone is aware of the fact that Revolution 4.0 has significantly changed our private lives. Almost all of us are already benefiting from technological advances called Industry 4.0. We are mobile, controlling devices at home remotely, keeping photos and files in the cloud, buying from online stores, receiving parcels from automated parcel machines, using online doctor consultations and wearing watches on our wrists that automatically upload sports performance data to the network, analyse it and provide reports. Our homes are cleaned by autonomous vacuum cleaners and the grass in front of the house is cut by wireless robot lawnmowers. Clothing and shoes are ordered without a traditional fitting using a virtual twin experience.

Revolution or evolution?

Revolution 4.0 as well as the three preceding ones represent a certain sequence of changes that have taken place in the world over the last 250 years. We might wonder whether we should call these changes a revolution, which by definition refers to changes that are sudden and reject the achievements of predecessors. In my opinion, a more appropriate word is "evolution", because nothing happened suddenly, the technological achievements of particular "revolutions" were implemented over the years. The same is true now as we have been talking loudly about Industry 4.0 for more than 10 years, and still many companies in Poland, especially the smaller ones, do not consider the implementation of the 4.0 as strategic or are at the stage of developing an implementation or pilot strategy. The implementation of Industry 4.0 is taking place evolutionally rather than by leaps since the absorption of new technologies is limited, and there are many barriers such as financial, mental or lack of skilled employees.

While we may wonder whether the technological changes occurring in the industry from Industry 1.0 to Industry 4.0 are revolutionary or evolutionary, the parallel changes in customer behaviour and expectations have been evolutionary.

Evolution of production systems

Simultaneously with technological advances over the years from Industry 1.0 to Industry 4.0, customer expectations have changed which, combined with the technological capabilities of factories, resulted in changes in production systems.

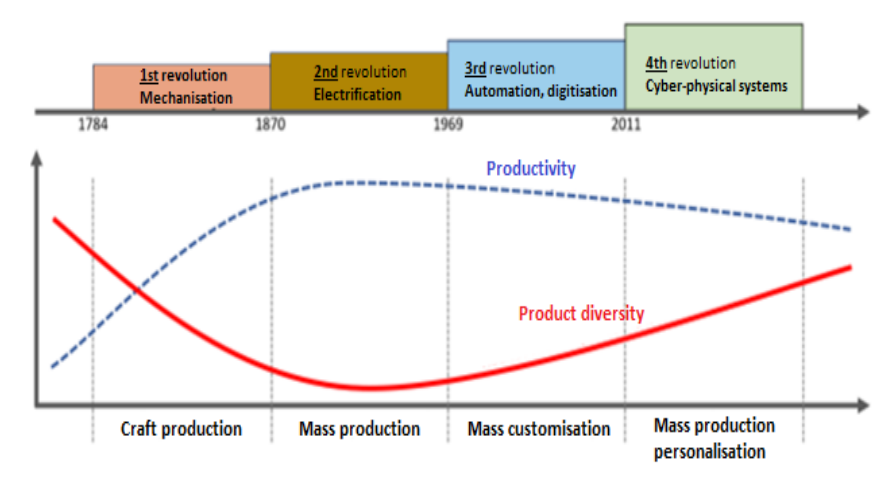


Figure 1. Evolution of production systems against the background of four industrial revolutions. Source: own study.

Industry 2.0 brought about the transition from artisanal to mass production, symbolised by the production of Ford cars in any colour as long they were black.

The mass production system resulted from the production capabilities of the factories at that time. For a product to be available to the customer it had to be mass-produced. Technologies used did not allow to production a personalised product at a low cost.

The next stage in the evolution of production systems was Industry 3.0. Automation and digitisation have allowed for more diverse production while retaining correspondingly high productivity. A conscious customer was no longer satisfied with a mass product, but was looking for a product tailored to their needs. The industry had to face this challenge and production entered the area of mass customisation.

Modern technologies of Industry 4.0 have made it possible to manufacture an even more diverse range of products at an acceptable cost level and adapt the product to the needs of a specific customer. The era of mass product personalisation has begun. The customer is no longer limited to choosing and buying, but is able to design a product for themselves using intuitive IT tools and product configurators.

To conclude, throughout four industrial revolutions, we can see a clear trend of moving from craft production through mass production and mass customisation to mass personalisation. This tendency is affecting more and more manufacturers, but of course, not all of them. The world is diverse, and so are customers, and there will probably be a demand for a mass-produced or even artisanal product all the time.

Mixed manufacturing environment

Together with the evolution of production systems, several other changes can be observed in the market. Globalisation increases the complexity of supply chains. Growing customer demands regarding comprehensive services lead to an expanded product range.

The outcome is that many companies operate in a mixed manufacturing environment, with a wide range of production, using many different technologies, multiple production systems and many types of production. At the same time, customised and personalised products are manufactured, products available upon request, large and small series, made to stock (MTS), made to order (MTO), assembled to order (ATO) or engineered to order (ETO).

Management systems in a mixed environment

Effective and efficient management in a mixed manufacturing environment is a major challenge and places new demands on both IT and organisational manufacturing systems. Concerning the wide variety of products, PLM systems for product lifecycle management are becoming increasingly important. The high level of complexity of production processes means that IT systems are no longer in the form of a simple pyramid of automation but are often connected with each other.

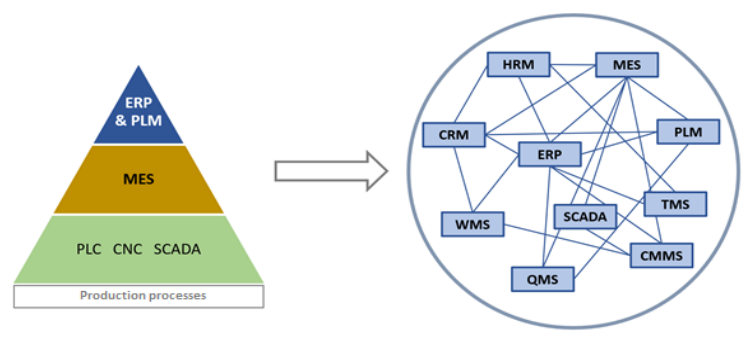


Figure 2. Complexity and interconnections of IT systems. Source: own study.

The ERP system does not cover all aspects of management, but begins to play the role of the main system combined with domain systems, specialised and adapted to the specifics of a particular product group, such as with many MES systems, each of which is intended for a different product group.

A mixed manufacturing environment also places new demands on organisational systems. The high level of complexity of the offer and the systems and production types used make planning and forecasting changes in demand, technological changes and several other factors very difficult. In such a situation, scalability, agility and flexibility become important requirements.

Scalability allows for easy, gradual increase and decrease of production capacities based on demand. This can be achieved by dividing processes into smaller modules, minimising dependencies between processes and splitting total production capacities into more devices.



Figure 3. Process scalability. Source: own study.

Agile and flexible production management is a key element in managing a mixed manufacturing environment. One of the systems supporting agility can be the Lean Manufacturing system that has been proved and well-established in many companies. Although this system is more associated with continuous improvement and waste elimination, it is, to some extent, a precursor of "agile" due to elements that improve agility such as fast changeovers, small series or one-piece flow. Despite the fact that the Lean system was created long before the "explosion" of the fourth industrial revolution, it works perfectly in today's complex manufacturing environment.

Mixed manufacturing environment at FAKRO

An example of production management in a mixed manufacturing environment can be FAKRO. The company's product range is very wide as it comprises a number of products such as wooden and PVC roof windows, flat roof windows, flashings, access roof lights, light tunnels, vertical windows, garage doors, smoke ventilation and control systems, Venetian blinds, external roller shutters and awning blinds, internal blinds.

The company employs a wide range of different technologies, including wood processing, plastic processing, glazing unit production and glass processing, varnishing and surface protection, sheet metal and profile processing, production of electronic components. FAKRO exports its products to more than 60 countries all over the world, in many cases customised according to the requirements of the market concerned. In certain product groups, for example vertical windows, all products are personalised. The roof window group includes both mass-produced products for stock as well as those customised and personalised according to customer expectations.

In a mixed manufacturing environment, with such technologically diverse products, applying one production system to all products becomes difficult and not optimal. Therefore, the company opted for dedicated systems tailored to the specifics of production and the equipment used. Two different systems can serve as an example: the first for the production of vertical windows and the second for the production of glazing units.

The increasing share of personalised products makes the company place great emphasis on the development of configurators so that the customer can easily personalise products according to their requirements. A major challenge for the company is the integration of configurators with production systems, because from the customer's point of view, configurators for different product groups should be similar or even the same, while taking into account production aspects, these are often diametrically opposed technologies and different production systems.

FAKRO applies the Lean Manufacturing philosophy in its production processes. The system was implemented in the first decade of this century while it was still in the "third revolution. Despite vital technological changes over the past several years and the emergence of Industry 4.0, the Lean system is still up-to-date and perfectly supports production management in a mixed manufacturing process.